R. & M. No. 3524

MINISTRY OF TECHNOLOGY

AERONAUTICAL RESEARCH COUNCIL
REPORTS AND MEMORANDA

A Piloted Simulator Study of the Take-off Manoeuvre of a Large Aircraft with and without a Take-off Director

By C. O. O'Leary and D. H. Perry

LONDON: HER MAJESTY'S STATIONERY OFFICE
1968

PRICE £1 0*s.* 0*d.* NET

A Piloted Simulator Study of the Take-off Manoeuvre of a Large Aircraft with and without a Take-off Director

By C. O. O'Leary and D. H. Perry

Reports and Memoranda No. 3524*
August, 1966

Summary.

A piloted simulation of the take-off manoeuvre of a large aircraft has been developed to aid research into take-off director instruments. Records of undirected take-offs made in real flight and on the simulator have been compared, and these, as well as pilot's subjective opinions, show that the simulation was adequate for its purpose. The need for cockpit motion and visual simulation was studied briefly.

Tests with one suggested form of take-off director showed that take-offs with the director were more consistent, and had increased margins of safety, compared with undirected take-offs.

CONTENTS

1. Introduction

2. The Simulation
   - 2.1. Special features of take-off simulation
     - 2.1.1. Computing
     - 2.1.2. Representation of the take-off to the pilot
   - 2.2. Initial setting up
   - 2.3. Subsidiary tests of the importance of simulation cues
   - 2.4. Pilots assessments of the take-off simulation
   - 2.5. Comparison between piloting techniques in the simulator and those in flight

3. Take-off Director Tests
   - 3.1. Take-off director control law used
   - 3.2. Test procedure
   - 3.3. Results and discussion
     - 3.3.1. The ground-run
     - 3.3.2. The flare-up and climb-out

4. Conclusions

References

Appendix A Equations of motion and computer block diagrams

Appendix B Simulator take-off conditions and their arrangement for each trial

*Replaces R.A.E. Tech. Report No. 66 244—A.R.C. 28 616.

Tables 1 to 7

Illustrations—Figs. 1 to 13

Detachable Abstract Cards

1. *Introduction.*

The increasing complexity of the take-off manoeuvre for large aircraft has created a growing interest in the development of instrument aids specially designed for this phase of flight[1]. Examples of such instruments are the take-off monitor and the take-off director. These developments have provided a new incentive to create a realistic simulation of aircraft dynamics and environment during take-off, for in this way preliminary testing and optimisation can be carried out relatively speedily and economically.

This Report describes a study which was made on the Aerodynamics Department piloted flight simulator at R.A.E. Bedford[2] in the spring of 1964, having the two main objectives:

(i) To demonstrate that a take-off simulation could be attained which was adequate, both on the criteria of pilot subjective opinion and by comparison with measured flight behaviour.

(ii) To assess the effectiveness of a control law which had been suggested for a take-off director instrument.

The aircraft simulated for this work was the Comet 3B, since actual take-off tests on this type had been made previously[3] at the R.A.E., thus enabling pilots to give reliable assessments of the simulation. Trace recordings of the flight take-offs were also available for direct comparison with those from the simulator.

The simulator computer was set up to represent both the longitudinal and lateral motions of the aircraft, from shortly after the start of the ground roll until it was established on a steady climb path. (The representation of the lateral motion on the ground was considerably simplified however.) A projected horizon and shadowgraph outline of a runway provided the pilot with a simplified impression of the view outside the aircraft to supplement the normal flight instrument indications. Cockpit motion in pitch and roll was also used. Varying conditions of wind and turbulence could be introduced for each take-off, so as to create a realistic degree of task difficulty, and engine failure at any stage of the take-off could be represented.

After some optimisation of the computation, so as to provide the best match between control response and dynamic behaviour in flight and on the simulator, a large number of simulated take-offs was performed under the various weather and engine failure conditions which could be represented. These trials formed the basis for comparison with both the previously measured flight trials and with the subsequent simulator tests of the take-off director. Finally, a few trials were made without the cockpit motion, and without the external visual simulation, in order to establish the importance of these cues for take-off work.

A description of the setting up and validation of the simulation is given in Section 2, while the tests of the take-off director instrument are reported in Section 3.

2. *The Simulation.*

2.1. *Special Features of Take-off Simulation.*

Take-off simulation poses a number of technical problems in addition to those generally met with in the simulation of flight away from the ground. These problems fall broadly into two categories: (a) computational, and (b) representational.

2.1.1. *Computing.* Three main factors lead to the increased computational complexity of the take-off simulation:

(1) The presence of ground restraints due to the undercarriage.

(2) The need to take into account large changes in aircraft speed and incidence.

(3) Non-linear aerodynamic effects due to ground interference.

The ground restraint due to the undercarriage may be dealt with in two ways. One method is to treat the take-off as comprising a 'ground running' phase and an 'airborne' phase, with separate sets of equations of motion which are switched at the instant of lift-off. The undercarriage itself may reasonably be considered as rigid, and the centre of rotation during the 'ground running' phase will be about the main wheels. The ground plane may then be considered as supplying a kinematic constraint to the aircraft's motion. Once the aircraft is airborne the conventional equations of motion for an aircraft, referred to an axis system through its centre of gravity, would be used.

The alternative method, used in the present simulation, is to keep the same set of equations throughout the take-off, (i.e. equations referred to the aircraft's c.g.), but to include terms in these equations which represent the forces and moments imposed on the aircraft by its undercarriage. For the purposes of pilot handling studies it is unnecessary to represent the undercarriage characteristics in any great detail – a simple spring and damper, appropriately limited, will usually prove sufficient. With this method the ground plane may be considered as supplying a force restraint to the aircraft's motion. This method was chosen because it bore a closer resemblance to the real physical system, and because it avoided the switching operation at the instant of lift-off.

The second factor mentioned above, the need to take account of large changes in aircraft speed and incidence, arose because it was considered desirable to simulate the whole take-off, from ground roll through to the steady climb out, even though the main interest in this exercise lay in the take-off rotation, and subsequent transition to the climb. The need to study the effects of early and late rotation also influenced the decision to represent large speed changes accurately. The main features involved were the non-linear variation of dynamic pressure with speed, and the variation of drag with incidence. The details are given in Appendix A.

As a further aid to computational accuracy the equations of motion were set up on the analogue computer so that the zero value of the voltage analogue for many of the variables corresponded roughly to the mid-point of their range. The whole swing from -100 volts to $+100$ volts was thus used, with a consequent improvement in the scaling. This also meant that the greatest errors in equipment linearity occurred in the regions of least interest – at the beginning of the ground roll, and at the end of the climb out. Full details are again given in Appendix A.

The third feature in which the take-off simulation differs from the simulation of flight away from ground is in the representation of aerodynamic interference effects, produced on the aircraft by its proximity to the ground. This whole subject is extremely complex, especially when the effects of the jet engine efflux are considered, and only a limited amount of wind tunnel and flight measured data for the Comet were available. This, combined with some theoretical estimates, allowed the effects of ground proximity on lift, pitching moment and A.S.I. error to be represented approximately, and these effects were found to have a considerable influence on the aircraft's handling.

2.1.2. *Representation of the take-off to the pilot.* The other main aspect of take-off simulation which must be considered is to determine what cues, in addition to his flight instruments, a pilot needs in order to make his behaviour in the simulator comparable with that in flight. Three sources of such cues were available in the present simulation:

(1) A simple shadowgraph display representing the pilot's view of the runway.

(2) Cockpit motion in pitch and roll.

(3) Noise and vibration to represent the rumble of the undercarriage.

A typical runway view provided by the shadowgraph projector is illustrated in Fig. 1, where the aircraft is depicted as being over the edge of the runway and banking back towards the centreline. The picture presented was of an infinitely long runway and there was no indication of forward speed. Lateral tracking, heading, and aircraft pitch and roll attitude changes were represented however, and this allowed the task of keeping straight on the runway during crosswind take-offs to be included in the simulation.

Cockpit motion in pitch and roll was provided by the mechanism shown in Fig. 2. The pilot's cockpit was some six feet ahead of the pitching pivot, so that he experienced some measure of the translational motion associated with pitching rotation about the main wheels on the real aircraft, although this effect was smaller in the simulator.

The effect of nose wheel rumble was created by regular inputs to the cockpit motion system, which represented the jolting of the wheel as it crossed the expansion joints between the separate slabs of concrete on the runway. The frequency of this nosewheel jolting was increased with aircraft speed, and its magnitude was made a function of the nose wheel reaction. The main wheel rumble was represented by audible noise which was cut off as the wheels left the ground.

The effectiveness of these additional cues in enhancing the realism of the simulation is discussed in Section 2.2.

The cockpit used for these tests was basically that of a small fighter or research type aircraft so that the overall environment was not very representative of that of a large transport aircraft. However it was possible to use a transport-aircraft type of control wheel, (Fig. 3) with representative movements and forces. In some of the tests it was necessary for a second 'crew member' to call out airspeeds during the take-off. This was done by one of the technical staff situated at a control desk outside the cockpit, but having a duplicate set of flight instruments before him.

2.2. *Initial Setting up*

During the initial stages of this investigation the main effort was directed towards providing a simulation that was sufficiently valid for evaluation of the take-off director, using the criteria:

(a) That the computer outputs from the simulator should match the measured behaviour of the aircraft in flight as closely as possible.

(b) That pilots should judge the simulator subjectively to be like the aircraft, and that their control actions during take-offs in the simulator should be similar to those in flight.

To this end all the simulation facilities available, such as cockpit motion and visual displays, were used from the outset. After the main programme had been completed however, a few subsidiary trials were made to establish the importance of the various cues in the overall effectiveness of the simulation.

The aerodynamic and other data used in representing the Comet 3B aircraft on the simulator were derived from several sources. Unpublished results from flight tests made at the R.A.E. provided the basic data for lift and pitching moment, with and without ground effect. These were used in conjunction with estimates made by the design firm, and with the results of wind-tunnel measurements, (unpublished).

During the initial evaluation of the simulation, pilots familiar with the Comet 3B aircraft complained that the rates of pitch resulting from elevator application during the take-off rotation were much larger than those experienced in flight. Comparison of recordings made in flight and on the simulator confirmed that this was so; for the 10 deg of up elevator usually used during the rotation, the pitch rates in flight were about 3 deg/sec, while those on the simulator were about 5 deg/sec. The reasons for this difference could not be found, and in order to provide a realistic representation of the aircraft for the take-off director work it was necessary to adjust the computation, in a fairly arbitrary way, until a good match between rotations made in flight and on the simulator was obtained. This involved reducing the elevator power from a value, $\frac{dC_M}{d\eta} = -0{\cdot}023$ per degree, to $\frac{dC_M}{d\eta} = -0{\cdot}0142$ per degree, and also changing the pitching characteristics from $\frac{dC_M}{d\alpha} = -0{\cdot}0168$ per degree to $\frac{dC_M}{d\alpha} = -0{\cdot}0142$ per degree. Although the latter values are given in the table of aerodynamic data, (Table 2), it should be emphasised that they have been arrived at in a fairly arbitrary way and their validity is therefore open to doubt.*

---

*Subsequent to these simulator tests a special series of flight measurements on the Comet 3B aircraft was made to establish the value of $\frac{dC_M}{d\eta}$ in free air. The value obtained was almost identical to that at first set up on the simulator, i.e. $\frac{dC_M}{d\eta} = -0{\cdot}023$ per degree. The reason for the different rotational behaviour of the real and simulated aircraft therefore remains something of a mystery. A possible explanation lies in the complex nature of the ground effect on pitching moment which may have been incorrectly represented.

During the investigation of this problem it was found that the ground effect on the aerodynamic characteristics altered the aircraft's rotational behaviour sufficiently for it to be very apparent to the pilot. This took the form of a marked hesitation in the rate of pitch, just before the aircraft became airborne. The physical explanation for this hesitation seems to lie in the enhanced nose down pitching moment variation with incidence, due to ground effect, which diminishes as the aircraft becomes airborne. It is illustrated in Fig. 4 which shows two simulated take-offs, one with and one without ground effect, together with a record from the flight tests.

Undercarriage rumble was not represented in the first few trials, and this led to complaints from the pilots that they had less indication of the progress of the ground roll, and in particular of nose wheel and main wheel lift-off, than was available to them in flight. Indications of nose wheel and main wheel rumble were therefore included, as described in Section 2.2, and this was felt to make the simulation much more realistic.

2.3. *Subsidiary Tests of the Importance of Simulation Cues.*

At the end of the main programme of tests, described in the following Section, a short subsidiary programme, was run to examine the importance of the visual and motion cues used in the simulation. This consisted of fifty simulated take-offs by three pilots. The director was not used during these tests, but the same crosswind and turbulence conditions as those represented in the main study were examined. Simulated take-offs were made, with and without cockpit motion, and with and without the external visual display, in a random order.

Examination of the trace recordings made during these tests showed that the pitch attitudes reached in the initial stages of the climb were consistently higher in the simulated take-offs made without motion, compared with those made with the motion cue. As a result, the climb-out speeds in the no-motion case were also consistently lower. Fig. 5 illustrates this effect, the mean attitude time history for thirteen take-offs without motion being compared with that for fifteen take-offs with motion. (Unfortunately the pitch attitudes reached in the no-motion tests were larger than had been anticipated, and the recorder reached its stops before the steady attitude was attained.)

More detailed examination of the time histories showed that there was no significant difference in the initial rates of rotation used in the simulation with and without motion. The larger attitudes achieved in the non-moving simulation occurred because the rotation into the climb-out attitude, after the aircraft had become airborne, was allowed to continue longer in this case.*

The sample flight record also shown in Fig. 5 suggests that the simulation with motion resulted in climb-out attitudes which were more representative of the real take-off behaviour.

As far as could be judged from a rather limited study, the presence, or otherwise, of the visual simulation made no detectable difference to the longitudinal control of the aircraft during rotation. However there is some evidence to show that both cockpit motion and the visual simulation affected the ease of lateral control during the crosswind take-off. Fig. 6 shows time histories of bank-angle variation immediately after unstick for three types of simulation; first with both motion and visual simulation; secondly with visual simulation only, and finally, with neither motion nor visual display. The number of runs made in each case was small, but there is an indication of greater difficulty in controlling the lateral motion in the last case, compared with the other two.

The conclusions regarding the importance of the motion and visual cues for longitudinal and lateral control, deduced from a study of the take-off time histories, were largely supported by the pilots' subjective judgments given below.

2.4. *Pilots' Assessments of the Take-off Simulation.*

Once the difficulties of achieving the correct rotation rate for a given stick movement, (described in 2.2), were overcome, pilots were, in general, favourably impressed with the realism of the simulation

*Subsequent simulation tests on the take-off manoeuvre of a large slender-wing transport aircraft have shown an even more marked difference between take-offs made with and without simulated cockpit motion.

and regarded it as entirely adequate for the take-off director assessment.

Their specific comments during the tests with different simulation cues supported the deductions from the time histories i.e.

(i) Without motion the pilot was far less conscious of the large pitch attitude achieved during climb out, and therefore tended to hold the rotational stick input on for longer than he would otherwise. One pilot said that the physical sensation of being at a large nose up attitude in the moving simulation made him much more concerned with speed control, and caused him to correct immediately any tendency for the speed to fall.

The visual simulation was felt to play only a small part in the longitudinal control. Initially it gave some indication of the rate of rotation, but the horizon rapidly dropped out of sight below the nose as the climb-out attitude was achieved.

(ii) In lateral control the effect of the different simulation cues was most evident in the crosswind take-offs, where the pilot had to contend with a rolling disturbance immediately after unstick. One pilot, when discussing the help provided by the visual and motion cues, said that both made the task of controlling the rolling motion very much easier, compared with the non-moving simulation with instruments alone. However, although the visual simulation gave a powerful indication of the aircraft's rolling motion, the correction of the motion still needed some thought and concentration, whereas with the moving simulation the correction was made quite instinctively and almost without any conscious effort.

(iii) In addition to the specific handling features where the simulation cues had a direct effect there was an overall impression that the cockpit motion, in particular, greatly enhanced the realism of the simulation and therefore affected the pilot's 'motivation' towards the simulation.

2.5. *Comparison between Piloting Techniques in the Simulator and those in Flight.*

As a means of establishing the validity of the simulation for the take-off director tests a detailed comparison has been made between a number of undirected take-offs performed on the simulator and those made on the Comet 3B aircraft. Fig. 7 shows superimposed time histories of several relevant variables, both from the simulation and from flight records. (These time histories have been arranged so that the aircraft always reaches the nominal rotation speed, V_R, at the same point on the time base.) Unfortunately circumstances prevented the same pilots from taking part in the take-offs used for this comparison although for both simulation and flight trials roughly half the take-offs were made by R.A.E. test pilots and half by airline pilots.

The take-off conditions represented on the simulator were always the same for these tests; a mean headwind of 10 knots, with turbulence, and at a uniform aircraft weight. As far as possible the flight trials chosen for comparison were made under similar conditions, but some variation was inevitable. As may be deduced from Fig. 7, this led to a variation of some 10 knots in the scheduled rotation speeds of the flight take-offs.

The general qualitative impression gained from Fig. 7 is of an encouraging similarity between the take-offs made on the simulator and those in flight. There are however a number of detailed features which deserve comment.

The records of elevator angle taken in the simulator trials show that two distinct techniques were used, one involving the gradual application of elevator several seconds before the rotation speed was reached, the other involving an abrupt elevator application at V_R. A similar distinction between gradual and abrupt elevator inputs is to be found in the flight time histories. It has been ascertained that, in every case, the gradual elevator applications were made by airline pilots, whilst the abrupt ones were made by the R.A.E. test pilots. No doubt this reflects a difference in the aims of the two groups of pilots. The airline pilots were asked, in both flight and simulator trials, to demonstrate the technique which they normally adopted in airline operations, while the R.A.E. test pilots had been told that they should try to achieve the lift off speed quoted in the flight manual, following rotation at a recommended speed 10 knots earlier. Previous experience had shown that a rather abrupt manoeuvre was necessary to achieve anything like these schedules.

After rotation all the time histories show a similar pattern, although there is noticeably more variability in the flight records, compared with those of the simulator. The consistency achievable in the

simulator, due no doubt to the exact repeatability of the conditions from run to run, the absence of distractions to the pilot, and the short time interval between successive take-offs, is a useful attribute during the initial development of an instrument such as the take-off director. However it is important that at some later stage the overall work load on the pilot should be made comparable to that which he experiences in flight, otherwise deficiencies in the system may not be revealed.

Fig. 7 shows only a few of the time histories recorded in the flight and simulator trials. Measurements made from a larger number of take-offs are shown in histogram form in Fig. 8. The parameters shown are: errors in rotation speed, maximum elevator angle used, maximum pitch rate achieved, and errors from the target unstick speed. The results of simple statistical tests on the data used for constructing the histograms of Fig. 8 are given in Table 5. (The number of measurements in each sample is not the same because some of the parameters were not recorded during every take-off.)

The tests show that both the mean error in rotation speed and its variability were noticeably lower on the simulator than in flight. The probable reasons for this greater consistency have already been mentioned. Elevator angles used, and maximum pitch rates achieved, were similar in flight and simulation, although there was more variability in the pitch rates measured in flight. Unstick-speed errors were lower on the simulator, as might have been expected from the lower errors in rotation speed, coupled with the similarity in pitch rates.

3. *Take-off Director Tests.*

Take-off measurements made during the Civil Aircraft Airworthiness Data Recording Programme and other studies of the take-off manoeuvre (e.g. Ref. 3) have shown that a reliable and accurate take-off director instrument is required to give the pilot sufficient aid to make significant improvements in precision and safety. The desirable qualities of such an instrument are discussed in Ref. 3 and these are summarised in the following extract from the M.O.A. specification for a take-off director[4]:

'The take-off director is required to increase the safety during take-offs and overshoots in modern aircraft by providing precise demands to the pilot in these manoeuvres; it will avoid the present need for him to correlate information from various instruments before deciding what action to take'.

'The take-off director is required to direct the pilot safely and accurately from the ground roll, through rotation, flare-up and the climb-out to at least 1500 ft, or through an overshoot from the minimum height. The director shall provide guidance in all phases of motion.'

Flight tests for developing and proving take-off directors are necessarily lengthy and expensive, and the tests described here illustrate the use of the flight simulator in accelerating the development programme.

3.1. *The Take-off Director Control Law used in the Tests.*

A take-off director control law, based on a pitch rate demand proportional to acceleration along the flight path, has been proposed by various bodies. The law used in the present experiment is based on one proposed by Elliott Bros. in an unpublished report. It is designed to provide pitch guidance through all phases of the take-off, and is displayed to the pilot on a flight director instrument, such as the F.4B Director/Horizon used in these tests. Fig. 3 shows the instrument situated in the middle of the instrument panel.

The operation of the director can best be explained by considering the three phases of operation separately:

Phase A – Initial ground run.

This phase covers the period from the start of the ground roll until rotation speed, V_R is reached. The pitch demand signal to the F.4B director is given by,

$$D_z = k_{\dot{\theta}}\dot{\theta} + k_v(V - V_R)$$

where $k_{\dot{\theta}}$ and k_v are constants. D_z is expressed as a percentage of full scale deflection. The $(V - V_R)$ component is suppressed until it is greater than -10 knots. Until the airspeed reaches $(V_R - 10)$ knots, the director target ring remains in a nose down demand position and responds to pitch rate about this

position (Fig. 9a). This assures the pilot that the director is 'live' when his task is mainly one of monitoring instruments and steering the aircraft down the middle of the runway. When the airspeed reaches $(V_R - 10)$ knots, the target ring moves up to give a decreasing nose down demand, reaching the null position at V_R (Fig. 9b). This acts as a warning to the pilots that he is reaching the speed at which he must initiate rotation.

Phase B – Rotation warning.

This phase commences when the speed reaches V_R. The director law is

$$D_z = k_{\dot\theta}\,\dot\theta + k_\theta\,(\theta - \theta_D)$$

where k_θ is a constant and θ_D is a preset demanded pitch attitude. At V_R the target ring 'kicks' up sharply from the null position as θ_D is switched in (Fig. 9c). The pilot commences rotation and seeks to bring the target ring back to the null position the director is nulled (Fig. 9d) when the demanded pitch rate is achieved, i.e. when $\dot\theta = -\dfrac{k_\theta}{k_{\dot\theta}}(\theta - \theta_D)$. During the rotation the demanded pitch rate is proportional to the attitude error from θ_D.

Phase C – After unstick.

This phase is switched in as the aircraft leaves the ground. The law is then

$$D_z = k_{\dot\theta}\,\dot\theta - k_v\left(\frac{1+8s}{1+s}\,V - V_D\right)$$

where s is the Laplace Transform variable and V_D is the demanded climb-out speed, and is given by:

$$V_D = V_2 + k_1\,(\dot h - k_2)$$

where k_1 and k_2 are constants, V_2 is the 'climb-out safety speed' and $\dot h$ is the rate of change of height. The demanded pitch rate during this phase is limited to 1·5 deg/sec.

The instrument directs the pilot to achieve a pitch rate which is proportional to the acceleration of the aircraft along the flight path, and then to hold a climb-out speed which is a function of the rate of climb. The transfer function $\dfrac{1+8^s}{1+^s}$ is designed to give phase advance on V, while filtering out the high frequency noise which results from differentiating an airspeed signal. In the simulation it was not practicable to reproduce accurately the effects of turbulence on differentiated airspeed, so that any deficiencies in the differentiating circuit would not have been apparent in the present tests.

Lateral guidance was also provided and comprised terms in heading, roll angle and roll rate which were summed in the form:

$$D_y = 3{\cdot}6\psi + 1{\cdot}25\dot\varphi + 3\varphi$$

where D_y is expressed as a percentage of full scale deflection. This lateral direction remained unchanged during the take-off, except for the period between unstick and 35 ft, when no heading corrections were demanded, so that the pilot was directed to keep the wings level near the ground.

All the control law gains and constants used during the tests were considered to be near the optimum by reference to performance and pilot opinion during the initial development testing.

The numerical values of the constants were as follows:

$k_{\dot\theta}$ 17 per cent f.s.d. per deg/sec rate of pitch

k_v 2·95 per cent f.s.d. per knot speed error

k_θ 8 per cent f.s.d. per deg pitch attitude error

θ_D 11 deg

k_1 1 knot per 120 ft/min rate of climb

k_2 1350 ft/min

3.2. *Test Procedure.*

The tests were divided into two sessions. The first set of trials consisted of undirected take-offs, in order that a flight/simulation comparison could be made, (*see* Section 2.5), and a basis established for assessing the effectiveness of the take-off director, which was used in the second set of trials.

A complete trial consisted of a nominal 20 take-offs by one pilot, although simulator malfunctions and pilot availability caused some trials to be considerably shorter. A range of take-off conditions was covered, including cross-wind, turbulence, and engine failure cases. The various combinations of parameters and their random order in the trials are detailed in Appendix B. Aircraft weight and centre of gravity position were as given in Table 1 and remained unchanged during the main programme. The normal take-off configuration was used, but the undercarriage and flaps were not retracted after unstick, and the target climb-out speed was somewhat lower than for normal operating procedure. This modified technique was adapted so that comparisons could be made with previous flight tests which had been conducted in this way[3].

Before each trial the pilot was briefed on the take-off power setting and elevator trim to be used, and before each take-off the conditions (of wind and turbulence) applicable were read out to him. Engine failure was also communicated to the pilot after it had been simulated; failures both at unstick and at 200 ft were represented.

For undirected take-offs, pilots used their normal visual and instrument techniques during all phases. During the ground run, speeds were called by the 'co-pilot' from 60 knots up to V_R. Apart from the rotation speed and the climb-out speed no other specific instructions were given to pilots regarding technique.

In directed take-offs, warning of V_R was given by a slow upward movement of the director target ring from its nose down demand position, and rotation was initiated when the target ring moved sharply upwards from the centre to give a nose up demand. Pilots were briefed to null the demand as rapidly as possible, consistent with accuracy, and to keep it nulled throughout the remainder of the take-off. It was left to the individual pilots to decide whether other instruments or visual cues should be used in addition to the director.

Each take-off lasted for approximately 2 minutes. Most of the analysis was concerned with a relatively short period after V_R, but speed holding during the climb-out was also of interest.

In a simulator running time of 24 hours a total of approximately 350 take-offs were performed, one third of which were directed. Some of these were for development purposes and were not recorded. The 9 pilots who participated in the trials were of varied backgrounds; they could be classified as follows:

A, B and C were test pilots very experienced in Comet take-offs,

D, E and F were test pilots without much experience in Comets,

G, H and J were airline pilots with previous Comet experience.

The recorded take-offs carried out by each pilot are given in Table 4. It was not possible for the same pilots to carry out the undirected and directed take-offs, but there was one (pilot A), who did do a substantial number of take-offs with and without the director, so that, in addition to the overall comparison of undirected and directed take-offs, an additional comparison was made for pilot A.

From the continuous trace records taken the following parameters were measured for each take off:

(i) Error in rotation speed, V_R.
(ii) Maximum elevator angle used during the rotation.
(iii) Maximum pitch rate during the rotation.
(iv) Unstick speed.
(v) Maximum lift coefficient.
(vi) Lift coefficients at 20 ft and 50 ft above ground level.
(vii) Airborne distance to reach a 35 ft screen height.

(viii) The mean modulus of the pitch and lateral director following errors on directed take-offs for a 100 sec period after V_R.

3.3. *Results and Discussion.*

The results are presented in the form of comparisons between undirected and directed take-off time histories (Figs. 10, 11 and 12), and histograms of significant parameters (Fig. 13a to j). Director-following errors are also examined for differences between pilots, and for the effects of turbulence, crosswind and engine failure (Tables 6 and 7). The ground run and airborne phases of the take-off will be discussed in separate sections.

3.3.1. *The ground run.* Since pitch-rate noise during the ground run was not presented on the director, the target ring remained steady in the nose down position and did not react to runway roughness. Warning of V_R was therefore clearly distinguished by the initial movement of the ring. In an aircraft system, pitch-rate noise would be superimposed on the signal and some damping would probably be required. Owing to an intermittent fault in the V_R trigger circuit the kick-up did not always occur at the scheduled speed, giving rise to a number of rotation-speed errors, of the order of 2 or 3 knots, which were additional to those due to the pilot, hence the unexpectedly large scatter in the histogram for directed take-offs shown in Fig. 13a. For the undirected take-offs the error limits are ± 8 knots, which is quite small compared with some operational measurements which have been made on airliners in service. It is though that insufficient work load, and a lack of distraction in the simulator, allowed pilots to concentrate almost exclusively on the ASI during the ground run, apart from which speeds were also being called out by the 'co-pilot'. Since pilots are under a much lower stress level in a simulator it would seem to be improbable that the use of a director would show any reduction in the variability of rotation speed.

Accuracy in achieving a given rotation speed should be simply a function of the pilots reaction time, if his entire concentration is directed towards this one object, and in these circumstances a needle moving over a scale will give much the same results as a kick up on the director. But when the pilot is under a high degree of stress the kick up on the director instrument would be expected to give a much stronger cue.

It is evident from Fig. 10 and Figs. 13b and c that rotation was less rapid when the director was used. Elevator deflections and pitch rates are seen to be of a generally lower level in the directed time histories and the histogram means of maximum elevator and pitch rate are also less. But the fact that the standard deviation of peak pitch rate is the same for both cases indicates that pilots were not able to improve on the variability of pitch rate during the rotation phase by using the director. Some error in the initial elevator input was inevitable, with the result that the initial pitch rate demand was not always satisfied. The rotation is a transient and unstable manoeuvre, and without actual direction of the stick movement required at V_R it would seem that consistently precise control of the initial rotation rate is difficult to achieve.

In the Flight Manual for the aircraft, unstick speeds are specified and pilots are recommended to initiate rotation 10 knots before unstick speed is reached. Since strict adherance to this procedure was found to encourage the application of unrealistically high pitch rates, pilots were instructed to initiate rotation at the specified speed and rotate at a reasonable rate, accepting somewhat higher unstick speeds. The time histories do not illustrate the effect well, but the histograms (Fig. 13d) show that unstick speeds were higher for directed take-offs, though there was no difference in standard deviation. The higher mean is accounted for by the lower pitch rates, and at least some of the scatter must have been due to the effect of the intermittent V_R triggering fault. It would seem that although it is probable that gross errors in unstick speeds can be avoided by using a director, a reduction in variability as measured in these tests could only be achieved with more precise direction during the initial rotation.

3.3.2. *The flare-up and climb-out.* These phases of the take-off will be discussed, firstly with reference to the basic four engine take-off in calm air, and secondly, with reference to the effects of turbulence, crosswind, engine failure and differences between pilots. Although the effects of turbulence and engine failure are illustrated separately in Figs. 11 and 12, the histograms in Fig. 13 include results with turbulence so as to give an overall picture of the variability.

Fig. 10 shows that use of the director reduced pitch oscillation, gave a much tighter control of pitch rate and pitch attitude, and led to a more prolonged hold of a constant rate of pitch. The flattening of some attitude traces at approximately 17 deg is not a genuine effect, as the limit of the recording paper was reached at this point.

Peak lift coefficients are seen to occur just after unstick in both the undirected and directed take-offs in Fig. 10, though Fig. 13e shows that maximum values were limited to a lower level in the directed take-offs. Also the 'Directed' histogram shows a desirable tendency towards skewness, which suggests a lower probability of exceeding an upper limit compared with the 'Undirected' histogram. Histograms of lift coefficient at 20 ft and 50 ft (Fig. 13f and g) have been drawn to assess how consistently the stall margin was maintained during these critical stages of the flare-up. There is no apparent effect due to the director at 20 ft, but at 50 ft reduced variability is evident, even though there were roughly half as many directed as undirected results. It might be expected that pilots would be following the director more accurately by 50 ft and achieving more consistency.

Only a slight reduction in the variability of the height-time histories is apparent in Fig. 10, but the variability of airborne distance to a 35 ft screen height is reduced, as shown in Fig. 13h, at least when results for all pilots are taken together. There appears to be no difference in the case of pilot A.

During the climb-out pilots experienced little difficulty in holding a constant speed. with or without the director, but they felt that the director considerably reduced the effort required.

The effects of turbulence are illustrated in the time histories of Fig. 11. Here too, the director enabled pilots to make more consistent take-offs, with generally the same pattern as in smooth air.

The effect of varied conditions on director-following errors is shown in Table 6, where four pilots did the take-offs for each condition. The errors have been normalised by expressing them as a ratio of the errors in smooth air. Pitch and lateral errors are not related. With turbulence the mean pitch error is seen to be doubled and the azimuth error considerably increased. With crosswind added, lateral errors were further increased but pitch errors were slightly reduced.

With engine failure at unstick, (Fig. 12), it is particularly evident that pilots improved their consistency of control by using the director. The difference in the variability of the undirected and directed time histories is quite marked, particularly in pitch rate and pitch attitude, which again show the influence of the director in helping the pilot to maintain a constant rate of pitch during the flare-up. Fig. 13j shows that the mean and standard deviation of distance to 35 ft were reduced; in fact the mean is little changed from the four engine case. The demanded pitch rate is limited to 1·5 deg/sec during the flare-up and since the drop in acceleration from the 4 to 3 engine case is not sufficient to reduce the demanded pitch rate to less than 1·5 deg/sec there is no significant change in the distance taken to reach 35 ft.

Table 6 shows that pitch director-following errors were not affected by engine failure, but lateral errors were considerably increased. This increase in lateral errors is most probably due to the effects of asymetric thrust.

The director-following errors of three pilots are compared in Table 7. The errors have again been normalised by expressing them as a ratio of the least pitch and lateral error respectively. The larger variation between the lateral errors suggests that pilots varied in the extent to which they concentrated on the lateral-following task, and there is evidence that pitch errors were reduced only at the expense of lateral accuracy. A contributary reason for this could well have been the interaction between pitch and azimuth error which is a serious deficiency of the F.4B Director Horizon in the take-off task. Pilots felt that separate pitch and azimuth director bars were desirable.

4. *Conclusions.*

(i) An adequate simulation of the take-off manoeuvre in a large aircraft was achieved. Representation of the external visual world appeared to be of secondary importance, but cockpit motion enhanced the realism of the simulation, improved pilots 'motivation' towards it, and resulted in the use of lower initial climb angles. There was also some slight evidence to suggest that both motion and visual simulation improved the lateral control task during a crosswind take-off.

Aerodynamic effects due to the presence of the ground were found to play a significant part in determining the aircraft's motion, underlying the need for more comprehensive measurements of these effects.

(ii) Undirected simulator take-offs compared fairly well with flight but there were some differences due to the lack of a realistic operational environment and inadequate pilot work load. Pilots tended to execute a more accurate manoeuvre in the simulator and take-offs were less variable, partly through decreased distraction and partly because simulator turbulence did not significantly affect the flight path.

(iii) The tests showed that useful results can be obtained in a simulator to aid the development of a take-off director. A comparison of undirected and directed simulator take-offs showed that, within the limitations of the simulation, use of the director improved consistency and increased the safety of critical stages of the manoeuvre. Peak values of lift coefficient were decreased without increasing the distance to a 35 ft screen height. On take-offs with engine failure at unstick both the mean and variance of distance to 35 ft were decreased when the director was used.

Owing to the differences in stress and work loads between this simulation and flight, it could not be expected that a director would cause major reductions in the variability of all take-off parameters. In future testing of take-off directors in simulators it would be desirable to increase the pilot work load.

REFERENCES

No.	*Author(s)*	*Title, etc.*
1	—	Symposium on aircraft take-off and landing problems. R.A.E. Report D.D.I., July 1963. A.R.C. 25 770.
2	D. H. Perry, L. H. Warton and C. E. Welbourn	A flight simulator for research into aircraft handling characterstics. R.A.E. Tech. Report 66 373, December 1966.
3	C. O. O'Leary, J. N. Cannell and R. L. Maltby	Take-off director tests on a transport aircraft including the use of a 'SCAT' take-off director. A.R.C. R. & M. 3508, April 1966.
4	—	Take-off and overshoot director system specification of requirements. Ministry of Aviation Nav 2b/TOD/1 Issue 3, May 1965.

APPENDIX A

Equations of Motion and Computer Block Diagrams.

A.1. *Equations of motion along the flight path* (*Fig. A1, A2*).

Drag.

The aerodynamic drag was computed from the relationship

$$D = qS\,C_D \tag{A.1}$$

and, for computational purposes, the variable qS was considered in the form:

$$qS = 100\,000 + \Delta qS \tag{A.2}$$

C_D, the drag coefficient was taken to be a function of incidence only for the fixed configuration used in the tests.

$$C_D = 0{\cdot}05 + 0{\cdot}00038\,\alpha^{o2} \text{ (from Table 2).}$$

The drag equation, scaled for analogue computation, was then

$$\left\{\frac{D}{150}\right\} = (1{\cdot}111)\{600\,C_D\} + (1{\cdot}111)\frac{1}{100}\left\{\frac{\Delta qS}{100}\right\}\{600\,C_D\} \tag{A.3}$$

with

$$\{600\,C_D\} = 30 + (0{\cdot}912)\frac{1}{100}\{5\alpha\}\{5\alpha\}. \tag{A.4}$$

Thrust.

The thrust per engine at full throttle was given by the relationship:

$$\text{Thrust} = 10\,500 - 5{\cdot}5\,V \text{ lb}$$

where V is the airspeed in knots.

To allow the representation of a single engine failure the computation of thrust was split in the proportion one quarter to three quarters, with appropriate switching to represent the engine failure. The scaled equation for analogue computation was:

$$\left\{\frac{T}{350}\right\} = (0{\cdot}90)\left\{\frac{t}{105}\right\} + (0{\cdot}30)^{*}\left\{\frac{t}{105}\right\} - (0{\cdot}126)\left\{\frac{V}{2}\right\}. \tag{A.5}$$

Motion along the flight path.

The overall equation for motion along the flight path was:

$$m\dot{V} = T\cos\alpha - D - W\sin\gamma. \tag{A.6}$$

---

*This term switched out on engine failure.

Taking the small angle approximation, $\cos\alpha = 1$ and $\sin\gamma = \frac{\gamma^0}{57{\cdot}3}$ and scaling for analogue computation.

$$\{20\dot{V}\} = (1{\cdot}40)\left\{\frac{T}{350}\right\} - (0{\cdot}60)\left\{\frac{D}{150}\right\} - (1{\cdot}33)\{5\gamma\}. \tag{A.7}$$

Indicated airspeed and dynamic pressure.

The aircrafts speed over the ground was obtained by integration of equation A.7. The relative airspeed was computed by adding the wind velocity v_w, which could comprise; (1) a steady wind component, (2) a wind component varying with height (wind shear), or (3) a random gusting wind component. These conditions could also be combined as noted in Appendix B.

The A.S.I. generally indicated relative airspeed, except close to the ground where a position error due to ground was represented. This error was such that the A.S.I. read 8 knots slow on the ground. This error was reduced, roughly as the inverse of the height, so that it was negligible at 50 feet.

For computational purposes the speed was represented by a perturbation, v, from a datum speed of 120 knots, so that:

$$\text{groundspeed } V = 120 + v \tag{A.8}$$

$$\text{airspeed } V_1 = 120 + v + v_w \tag{A.9}$$

The dynamic pressure was computed from the relationship $q = \frac{1}{2}\rho V_i^2$, where ρ was taken to be constant at the standard sea level value, 0·00238 slug/cu ft. Combining A.2 and A.9, the scaled equation for analogue computation of ΔqS was:

$$\left\{\frac{\Delta qS}{1000}\right\} = 0{\cdot}80 + (1{\cdot}68)\{v + v_w\} + (0{\cdot}70)\frac{1}{100}\{v + v_w\}\{v + v_w\}. \tag{A.10}$$

A.2. *Equations of motion normal to the flight path* (*Fig.* A.3, *A.4*).

Lift.

The aerodynamic lift was computed from the relationship

$$L = qS\,C_L \tag{A.11}$$

where, for the fixed configuration tested, C_L was taken to be a function of incidence, wheel height, and elevator angle. From the data given in Table 2.

$$C_L = 0{\cdot}3 + 0{\cdot}065\alpha + \frac{0{\cdot}175(\alpha + 4{\cdot}5)}{h + 7{\cdot}4} - 0{\cdot}0082\eta \text{ (α and η in degrees).} \tag{A.12}$$

For computational purposes the lift was written in the perturbation form:

$$L = 100\,000 + \Delta L \tag{A.13}$$

giving the scaled equation

$$\left\{\frac{\Delta L}{1000}\right\} = (1{\cdot}428)\{70C_L\} + (1{\cdot}428)\frac{1}{100}\left\{\frac{\Delta qS}{1000}\right\}\{70C_L\} - 100 \tag{A.14}$$

with

$$\{70C_L\} = 21+(0{\cdot}91)\{5\alpha\}+\frac{100}{\{2h+14{\cdot}8\}}[(0{\cdot}0492)\{5\alpha\}+1{\cdot}10]-(0{\cdot}115)\{5\eta\}. \tag{A.15}$$

Wheel reactions.

The main wheel reactions assumed to result from a simple spring and damper were based on the assumed combined oleo stiffness of 120 000 lb/ft. The oleo compression was given by

$$\text{main oleo compression} = -h+l_m\frac{\theta^o}{57{\cdot}3} \tag{A.16}$$

where h height of aircraft c.g. above ground static position

l_m horizontal distance from c.g. to main wheels

θ aircraft attitude

in addition an arbitrary damping term, proportional to $\dot{h}$ was represented.

For computational purposes the main wheel reaction was considered in the form

$$R = 100\,000+\left\{\frac{\Delta R}{1000}\right\}\text{lb} \tag{A.17}$$

and the scaled equation for computing the perturbation in wheel reaction was

$$\left\{\frac{\Delta R}{1000}\right\} = -(60)\{2h\}+(1{\cdot}25)\{4\theta\}-(60)\{\dot{h}\}. \tag{A.18}$$

The nose wheel reactions were based on an assumed oleo stiffness of 10 000 lb/ft. The expression for oleo compression was similar in form to A.16, above, but the arbitrary damping term was dependent both on $\dot{h}$ and $\dot{\theta}$.

The scaled equation for nose wheel reaction was

$$\left\{\frac{r}{200}\right\} = 27{\cdot}5-(25)\{2h\}-(10)\{4\theta\}-(25)\{\dot{h}\}-(0{\cdot}54)\{10\dot{\theta}\}. \tag{A.19}$$

Special arrangements were necessary to ensure limiting of the computed wheel reactions to positive or zero values. In the case of the main wheels this involved a relay device which locked the perturbation in ΔR to a value of $-100\,000$ lb whenever the value computed from equation A.18 was more negative. For the nose wheel reaction the value of r was held at zero whenever equation A.19 yielded a negative value.

Motion normal to the flight path.

The overall equation for motion normal to the flight path was:

$$mV\dot{\gamma} = L-W\cos\gamma+R+r+T\sin\alpha \tag{A.20}$$

Taking the small angle approximation $\cos\gamma = 1-\frac{1}{2}\left(\frac{\gamma^o}{57{\cdot}3}\right)^2$ and $\sin\alpha = \frac{\alpha^o}{57{\cdot}3}$, the scaled equation for

analogue computation was

$$\{20\dot{\gamma}\} = \frac{100}{\left\{\frac{V}{2}\right\}}\left[120{\cdot}5+(1{\cdot}15)\left\{\frac{\Delta L}{1000}\right\}+(0{\cdot}066)\frac{1}{100}\{5\gamma\}\{5\gamma\}+(1{\cdot}15)\left\{\frac{\Delta R}{1000}\right\}\right.$$

$$\left.+(0{\cdot}230)\left\{\frac{r}{200}\right\}+(0{\cdot}14)\frac{1}{100}\left\{\frac{T}{350}\right\}\{5\alpha\}\right]. \qquad \text{(A.21)}$$

The climb angle, γ, was obtained by integration of A.21 and hence the rate of climb was derived from the small angle approximation:

$$\dot{h} = V\frac{\gamma^o}{57{\cdot}3}. \qquad \text{(A.22)}$$

A.3. *Equations of motion for pitching rotation (Fig. A.5, A.6).*

Pitching moment.

The aerodynamic pitching moment was computed from the expression:

$$M_A = qSc\,C_{M_S}+\frac{\rho VScl}{4}\left[\frac{dC_M}{d\left(\frac{\dot{\theta}l}{2V}\right)}\dot{\theta}+\frac{dC_M}{d\left(\frac{\dot{\alpha}l}{2V}\right)}\dot{\alpha}\right] \qquad \text{(A.23)}$$

C_{M_S}, the 'static' pitching-moment coefficient was taken to be a function of incidence, wheel height and elevator for the fixed configuration tested. From data given in Table 2

$$C_{M_S} = 0{\cdot}0299-0{\cdot}0142\alpha-\frac{0{\cdot}0665\alpha}{h+7{\cdot}4}-0{\cdot}0142\eta \text{ (α and η in degrees).} \qquad \text{(A.24)}$$

The corresponding scaled equations for the analogue computation were:

$$\left\{\frac{M_A}{5000}\right\} = (0{\cdot}956)\{400C_{M_S}\}+(0{\cdot}956)\frac{1}{100}\{400C_{M_S}\}\left\{\frac{\Delta qS}{1000}\right\}$$

$$+\left\{\frac{V}{2}\right\}\frac{1}{100}[(0{\cdot}121)\{20\dot{\gamma}\}-(0{\cdot}785)\{10\dot{\theta}\}] \qquad \text{(A.25)*}$$

where

$$\{400C_{M_S}\} = 11{\cdot}95-(1{\cdot}322)\{5\alpha\}-\frac{100}{\{2h+14{\cdot}8\}}(0{\cdot}106)\{5\alpha\}-(1{\cdot}84)\{5\eta\}. \qquad \text{(A.26)}$$

Moments due to wheel reactions.

These may be expressed by the equation

$$M_R = l_N r - R\left(l_M-\frac{\alpha^o}{57{\cdot}3}h_{cg}\right)$$

*n.b. For convenience this expression uses $\dot{\alpha} = \dot{\theta}-\dot{\gamma}$.

where l_N, l_M are the horizontal distances of nose and main wheels from the aircraft c.g., and h is the height of the c.g. above the ground.

The scaled equation for the analogue computation is:

$$\left\{\frac{M_R}{5000}\right\} = (1{\cdot}73)\left\{\frac{r}{200}\right\} - 53{\cdot}2 - (0{\cdot}532)\left\{\frac{\Delta R}{1000}\right\} + (0{\cdot}628)\{5\alpha\}$$

$$+(0{\cdot}628)\frac{1}{100}\left\{\frac{\Delta R}{1000}\right\}\{5\alpha\}. \tag{A.27}$$

Equation for pitching rotation.

The overall equation for pitching acceleration was:

$$B\ddot{\theta} = M_A + M_R + T\,Z_T \tag{A.28}$$

where Z_T is the distance of the thrust line below the c.g. Rate of pitch and pitch attitude were obtained by successive integration of equation A.28.

The angle of incidence was computed from the expression:

$$\alpha = \theta - \gamma + \alpha_o + \alpha_g \tag{A.29}$$

where α_o wing setting angle to the body datum

α_g incidence variations due to random gusts

A.4. *Equations for rolling and yawing motion (Fig. A.7).*

Since the task under investigation was predominantly one concerned with longitudinal control, the representation of the aircraft's lateral behaviour was less detailed. It was intended to provide sufficient realism to allow the added difficulties of taking off in lateral disturbances to be studied.

The rolling moments acting on the aircraft were represented by the equation:

$$L = qSb\,(l_\xi\,\xi + l_v\,\beta) + \frac{\rho V S b^2}{4}(p\,l_p + r\,l_r). \tag{A.30}$$

After scaling and substituting the values of the lateral derivatives given in Table 2, this becomes

$$\left\{\frac{L}{10000}\right\} = -(0{\cdot}45)\{5\xi\} - (0{\cdot}45)\frac{1}{100}\left\{\frac{\Delta qS}{1000}\right\}\{5\xi\} - (0{\cdot}292)\{8\beta\}$$

$$-(0{\cdot}292)\frac{1}{100}\left\{\frac{\Delta qS}{1000}\right\}\{8\beta\} - (0{\cdot}635)\frac{1}{100}\{5p\}\left\{\frac{V}{2}\right\}$$

$$+(0{\cdot}234)\frac{1}{100}\{10r\}\left\{\frac{V}{2}\right\}. \tag{A.31}$$

The yawing moments acting on the aircraft were given by

$$N = qSb\,(n_\zeta\,\zeta + n_v\,\beta) + \frac{\rho V S b^2}{4}(p\,n_p + r\,n_r) + \Delta T\,y_T \tag{A.32}$$

where the term $\Delta T\,y_T$ represents the yawing moment produced by an engine failure.

After scaling and substituting the values of the lateral derivatives given in Table 2, this becomes:

$$\left\{\frac{N}{5000}\right\} = -(0{\cdot}484)\{4\zeta\} - (0{\cdot}484)\frac{1}{100}\{4\zeta\}\left\{\frac{\Delta qS}{1000}\right\} + (0{\cdot}379)\{8\beta\}$$
$$+(0{\cdot}379)\frac{1}{100}\{8\beta\}\left\{\frac{\Delta qS}{1000}\right\} - (0{\cdot}268)\frac{1}{100}\left\{\frac{V}{2}\right\}\{5p\}$$
$$-(0{\cdot}226)\frac{1}{100}\left\{\frac{V}{2}\right\}\{10r\} - (0{\cdot}242)\left\{\frac{T}{350}\right\}^{*}. \tag{A.33}$$

*switched in on engine failure.

The rates of roll and yaw resulting from these moments were found by integration of the expressions:

$$\dot{p} = L/I_A \quad \dot{r} = N/I_C. \tag{A.34}$$

A.5. *Equations for sideslipping motion (Fig. A.8).*

The angular velocity of the flight path normal to the aircraft's plane of symmetry is given approximately by:

$$R_W = \frac{1}{mV}\left(2qSy_v\beta + mg\frac{\phi^o}{57{\cdot}3}\right). \tag{A.35}$$

After scaling and substitution of the appropriate derivative this becomes:

$$\{25R_W\} = \frac{100}{\left\{\frac{V}{2}\right\}}\left[-(0{\cdot}117)\{8\beta\} - (0{\cdot}117)\frac{1}{100}\{8\beta\}\left\{\frac{\Delta qS}{1000}\right\} + (0{\cdot}60)\{4\phi\}\right] \tag{A.36}$$

The angle of sideslip is obtained as the difference between heading and track in still air:

$$\{8\beta\} = (4)\{2\chi\} - (4)\{2\psi\} \tag{A.37}$$

with additional terms added to represent cross winds and lateral gusting.

APPENDIX B

Simulator Take-off Conditions and their Arrangement for each Trial.

Description of condition	*Code*
10 knots headwind, 4 engines	a
Engine failure at unstick	b
Engine failure at 200 ft	c
Turbulence (mild, $1\frac{1}{2}$ ft/s r.m.s. longitudinal and vertical, 3 ft/s r.m.s. lateral)	d
20 knots crosswind component	e
Wind shear, 10 knots at zero ft to 30 knots at 50 ft	f
Wind shear, 20 knots crosswind component at 50 ft	g

For each trial the above conditions were mixed in the following random order:

Runs	
1, 16, 19	a
2	a b
9	a c
3, 12, 18	a d
5, 13	a b d
11, 14	a c d
8, 15, 17, 20	a d e
6	a d f
4	a d g
7	a b d e
10	a c d e

TABLE 1

General Data Relating to the Comet 3b Aircraft Simulated.

Weights and inertias.	
A.U.W.	95 000 lb
Mass	2950 slug
Pitching inertia	1 000 000 slug-ft^2 ($I_B = 0{\cdot}131$)
Rolling inertia	1 302 500 slug-ft^2 ($I_A = 0{\cdot}153$)
Yawing inertia	2 260 000 slug-ft^2 ($I_C = 0{\cdot}266$)
C.G. position	$0{\cdot}25\ \bar{c}$
Areas, dimensions, etc.	
Wing area	2059 sq ft
Span	107·6 ft
Chord (S.M.C.)	19·15 ft
Tail arm	50·73 ft
Main wheel position	$0{\cdot}375\ \bar{c}$
Nose wheel position	$-2{\cdot}01\ \bar{c}$

TABLE 2

Aerodynamic Data used to Represent the Comet 3b Aircraft.

(Configuration: Flaps 20°/20° undercarriage down)

1 *Variation of lift, drag and pitching moment with incidence, away from the ground:*

$$C_L = 0{\cdot}3 + 0{\cdot}065\alpha^\circ$$

$$C_D = 0{\cdot}05 + 0{\cdot}00038\alpha^{\circ 2}$$

$$C_M = 0{\cdot}0299 - 0{\cdot}0142\alpha^\circ$$

2 *Change in lift and pitching moment* due to ground effect (change in drag due to ground effect neglected).*

$$\Delta C_{L_G} = \frac{0{\cdot}175\,(\alpha^\circ + 4{\cdot}5)}{h + 7{\cdot}4}$$

$$\Delta C_{M_G} = -\frac{0{\cdot}0665\alpha^\circ}{h + 7{\cdot}4}$$

3 *Elevator power**

$$\frac{dC_M}{d\eta} = -0{\cdot}0142 \text{ per } ^\circ$$

$$\frac{dC_L}{d\eta} = -0{\cdot}0082 \text{ per } ^\circ$$

4 *Damping derivatives.*

$$\frac{dC_M}{d\left(\frac{\dot{\theta} l}{2V}\right)} \left[\equiv \frac{4l}{57{\cdot}3\bar{c}} m_q \right] = -0{\cdot}0671 \text{ per deg.}$$

$$\frac{dC_M}{d\left(\frac{\dot{\alpha} l}{2V}\right)} \left[\equiv \frac{4l}{57{\cdot}3\bar{c}} m_{\dot{w}} \right] = -0{\cdot}0298 \text{ per deg.}$$

5 *Lateral derivatives (assumed constant).*

$$y_v = -0{\cdot}207$$

$$y_\zeta \quad \text{neglected}$$

$$l_p = -0{\cdot}380$$

$$l_r = +0{\cdot}281$$

$$l_v = -0{\cdot}124$$

$$l_\xi = -0{\cdot}1198$$

$$l_\zeta \quad \text{neglected}$$

$$n_p = -0{\cdot}08$$

$$n_r = -0{\cdot}1351$$

$$n_v = +0{\cdot}0808$$

$$n_\xi \quad \text{neglected}$$

$$n_\zeta = -0{\cdot}0515$$

*see Note in Section 2.2 concerning these parameters.

TABLE 3

Miscellaneous Data used in the Simulation.

1 *Elevator gearing.*
Shown in Fig. A.5.

2 *Ground effect on A.S.I. reading.*

A.S.I. error $= \dfrac{-59}{h+7{\cdot}4}$ knots.

(empirical relationship devised to give an error of -8 knots on the ground, and the same variation with height as ΔC_{L_G}).

3 *Undercarriage stiffness.*

Stiffness of main-wheel undercarriage (per side)	60 000 lb per ft
Stiffness of nose-wheel undercarriage	10 000 lb per ft

TABLE 4

Number of Recorded Take-offs by each Pilot.

Pilot	Undirected	Directed
A	60	20
B	20	0
C	20	7
D	19	0
E	0	26
F	0	28
G	5	0
H	5	0
J	20	0

TABLE 5

Statistical Comparison of Simulator and Flight Undirected Take-offs.

S = simulator

F = flight

Quantity	Number of occasions		Mean		Standard deviation or (variance)$^{\frac{1}{2}}$		Is the distribution normal?		Is the difference in MEANS significant?	Is the difference in VARIANCE significant?
	S	F	S	F	S	F	S	F		
Error in rotation speed kt	127	58	0·2	2·5	2·5	3·8	No	Yes	Yes	Yes
Maximum up-elevator used deg	144	65	9·6	9·8	0·9	1·1	No.	Yes	No	No
Maximum pitch rate deg/sec	145	58	3·3	3·5	0·61	0·89	Yes	Yes	No	Yes
Error in unstick speed kt	86	58	5·0	6·1	7·8	9·8	No	Yes	Yes	No

TABLE 6

Director Following Errors in Varying Simulator Conditions.

Number of take-offs	Code	Conditions	Mean modulus errors	
			Pitch	Lateral
8	a	Smooth, 10 kt headwind	1	1
8	ad	Turbulent, 10 kt headwind	2·2	1·6
11	ade	Turbulent, 10 kt headwind, 20 kt crosswind component	2·0	2·0
8	abd	Turbulent, 10 kt headwind, engine failure at unstick	1·9	2·4

TABLE 7

Comparison of Three Pilot's Director-Following Errors.

Pilot	Number of take-offs	Mean modulus errors	
		Pitch	Lateral
A	9	1·10	1·00
E	9	1·03	1·17
F	9	1·00	1·33

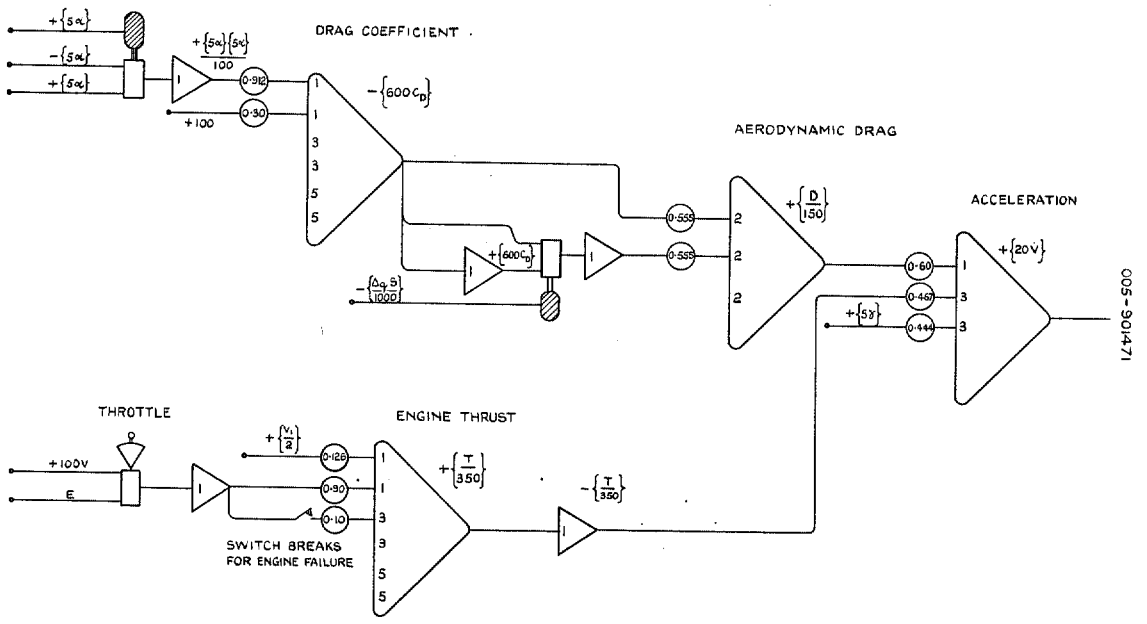

FIG. A.1. Motion along the Flight Path 1.

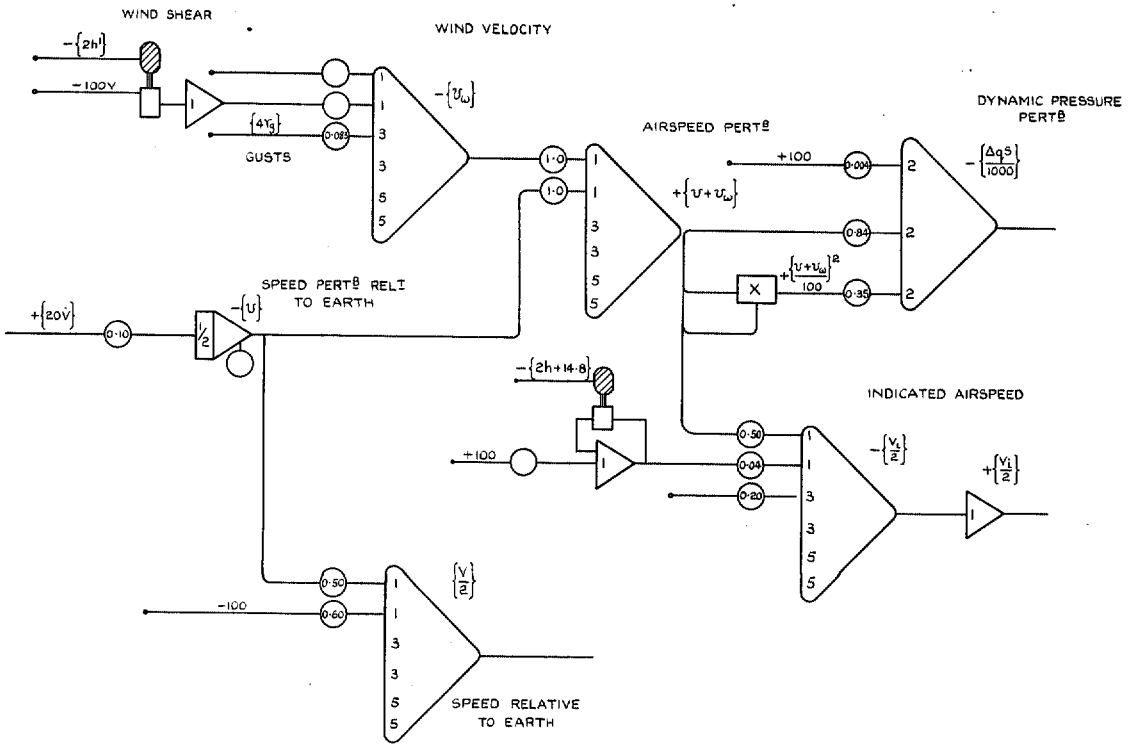

FIG. A.2. Motion along the Flight Path 2.

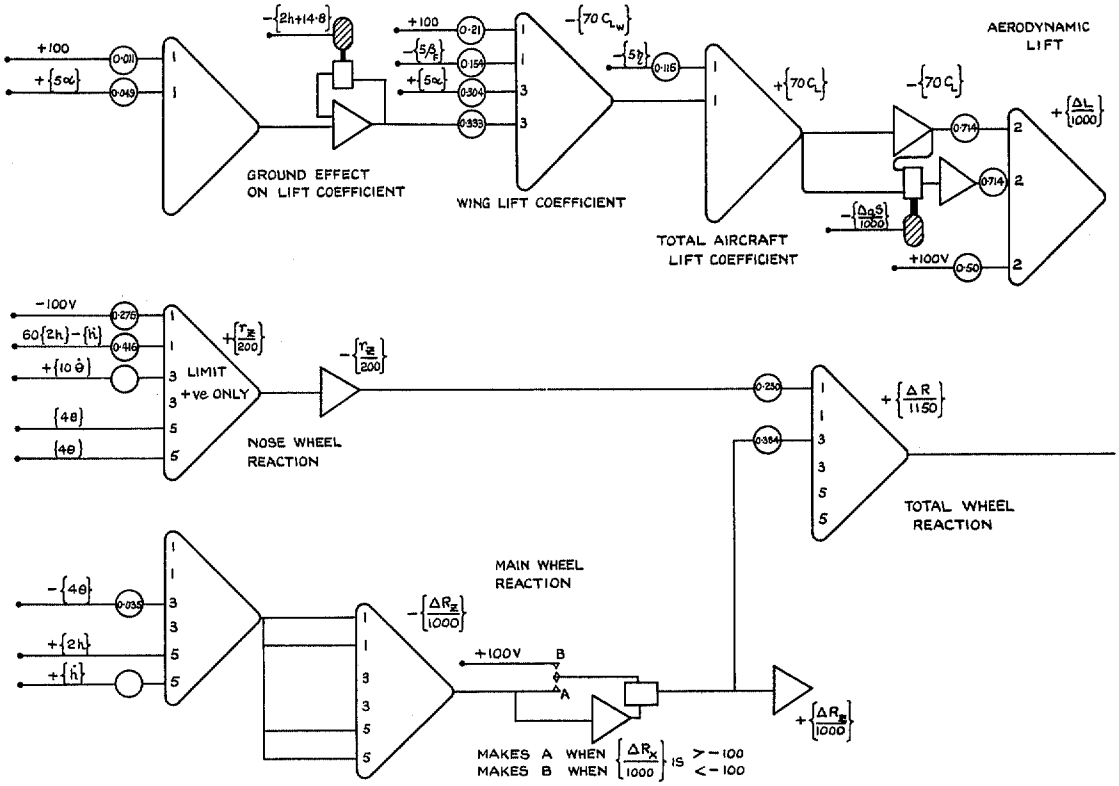

FIG. A.3. Motion normal to Flight Path 1.

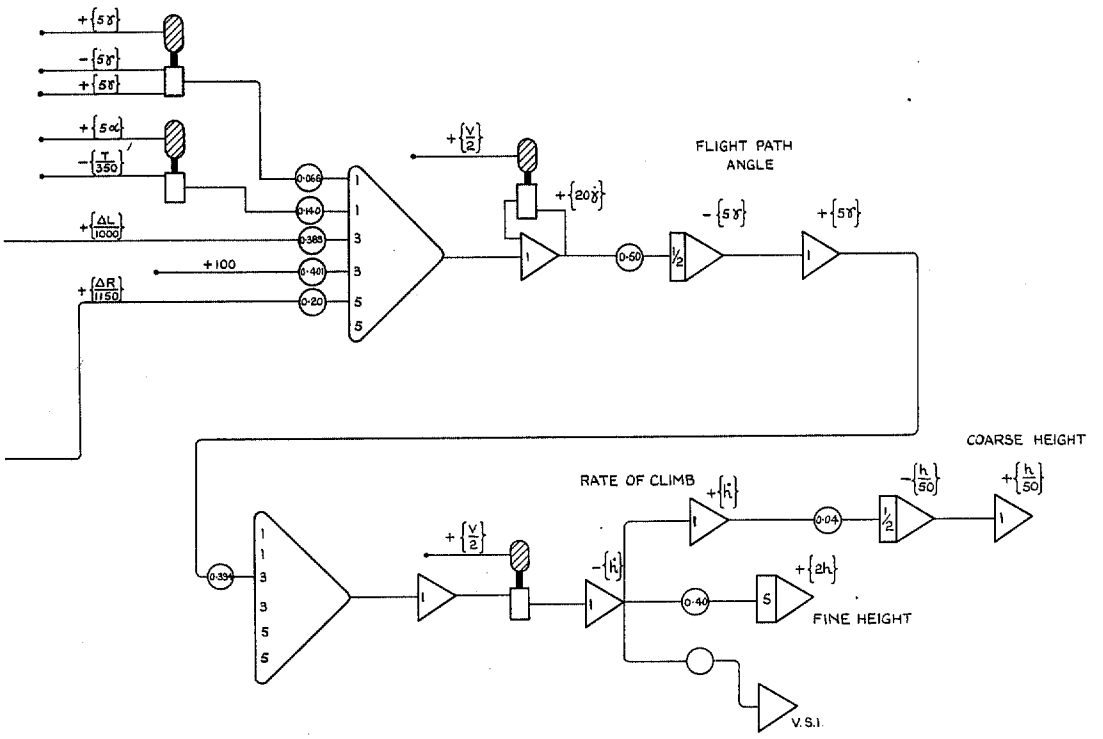

FIG. A.4. Motion normal to Flight Path 2.

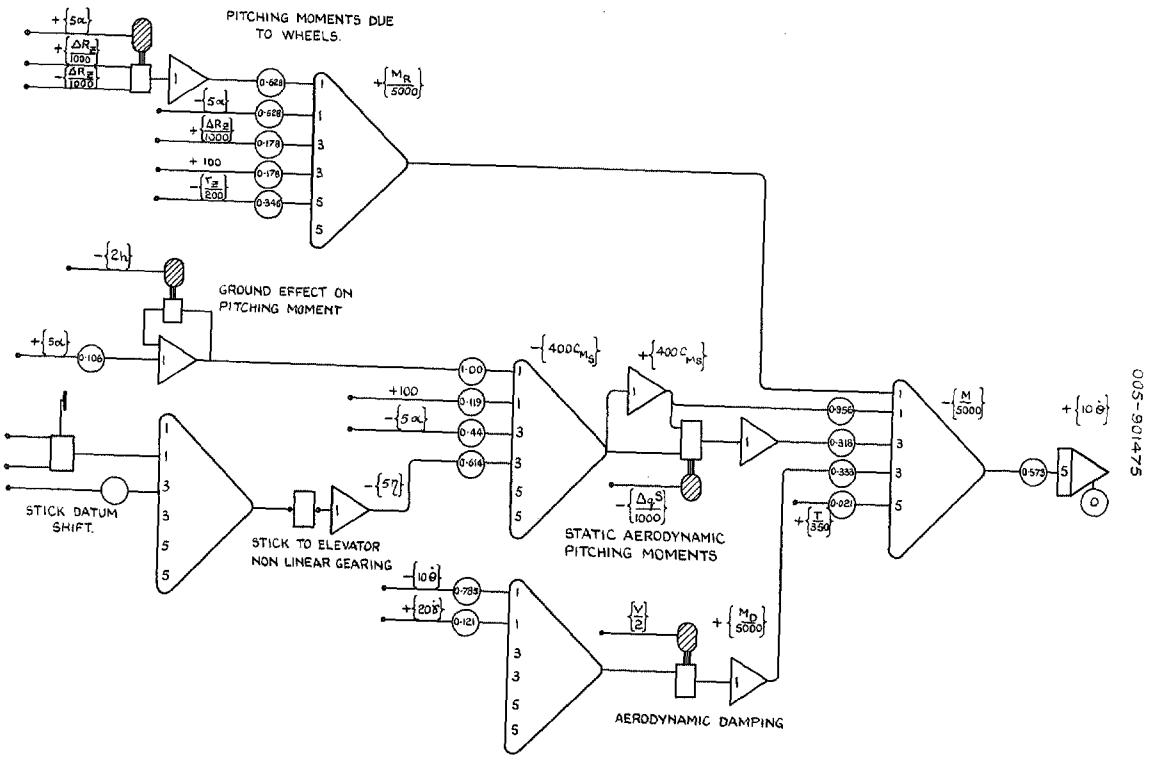

FIG. A.5. Pitching motion about the c.g. 1.

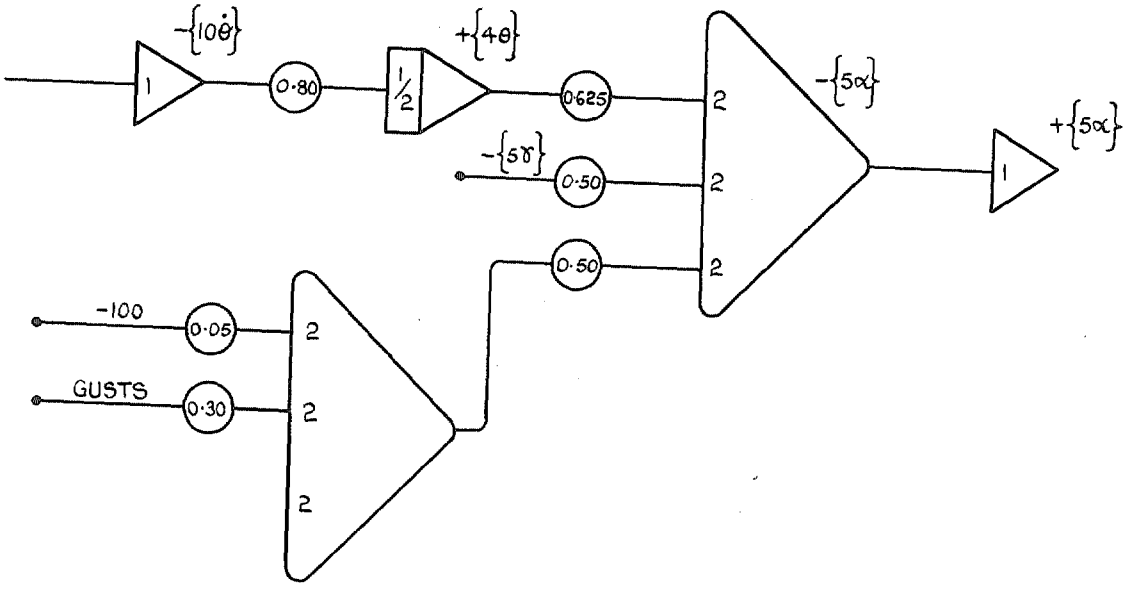

FIG. A.6. Pitching motion about the c.g. 2.

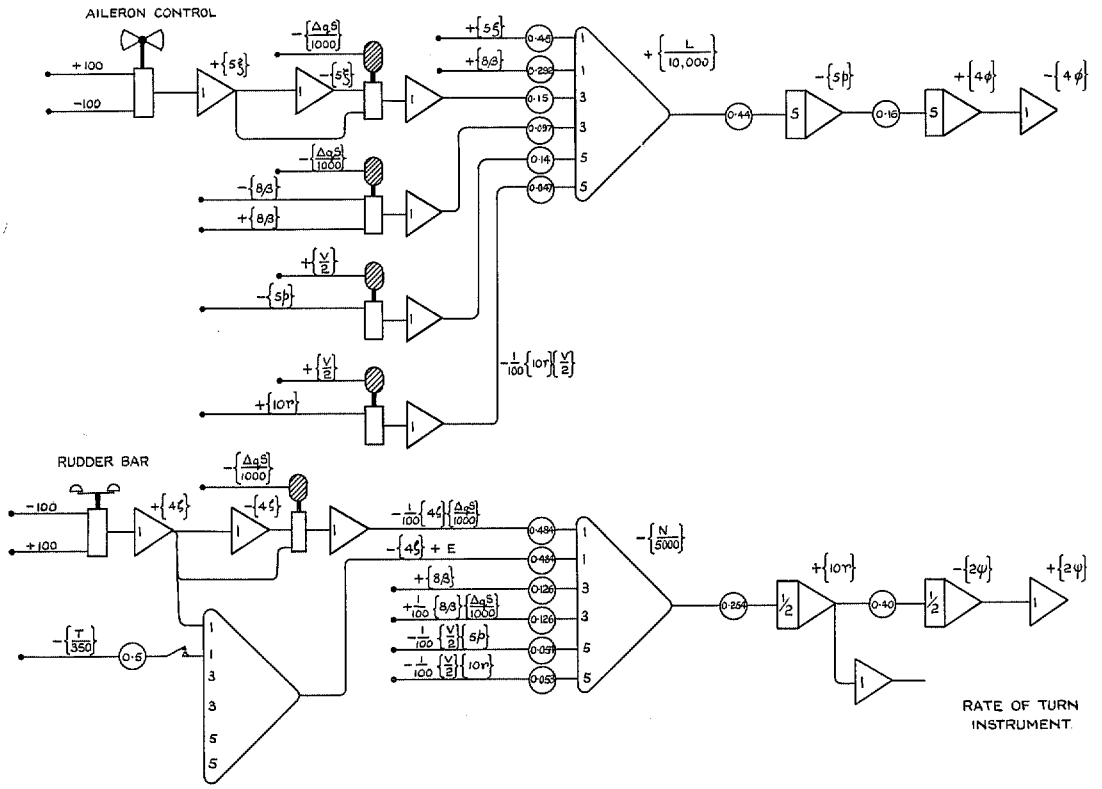

FIG. A.7. Lateral motion – rolling and yawing.

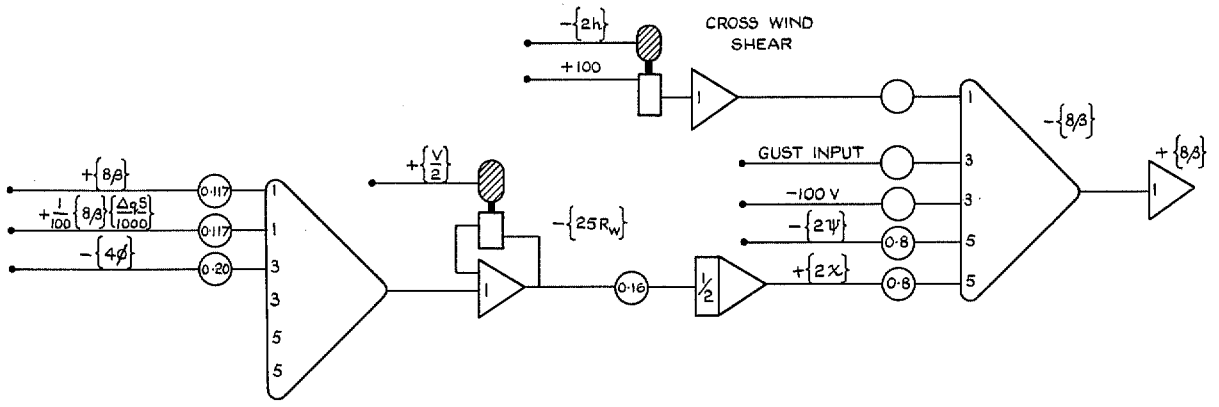

FIG. A.8. Lateral motion – sideslipping.

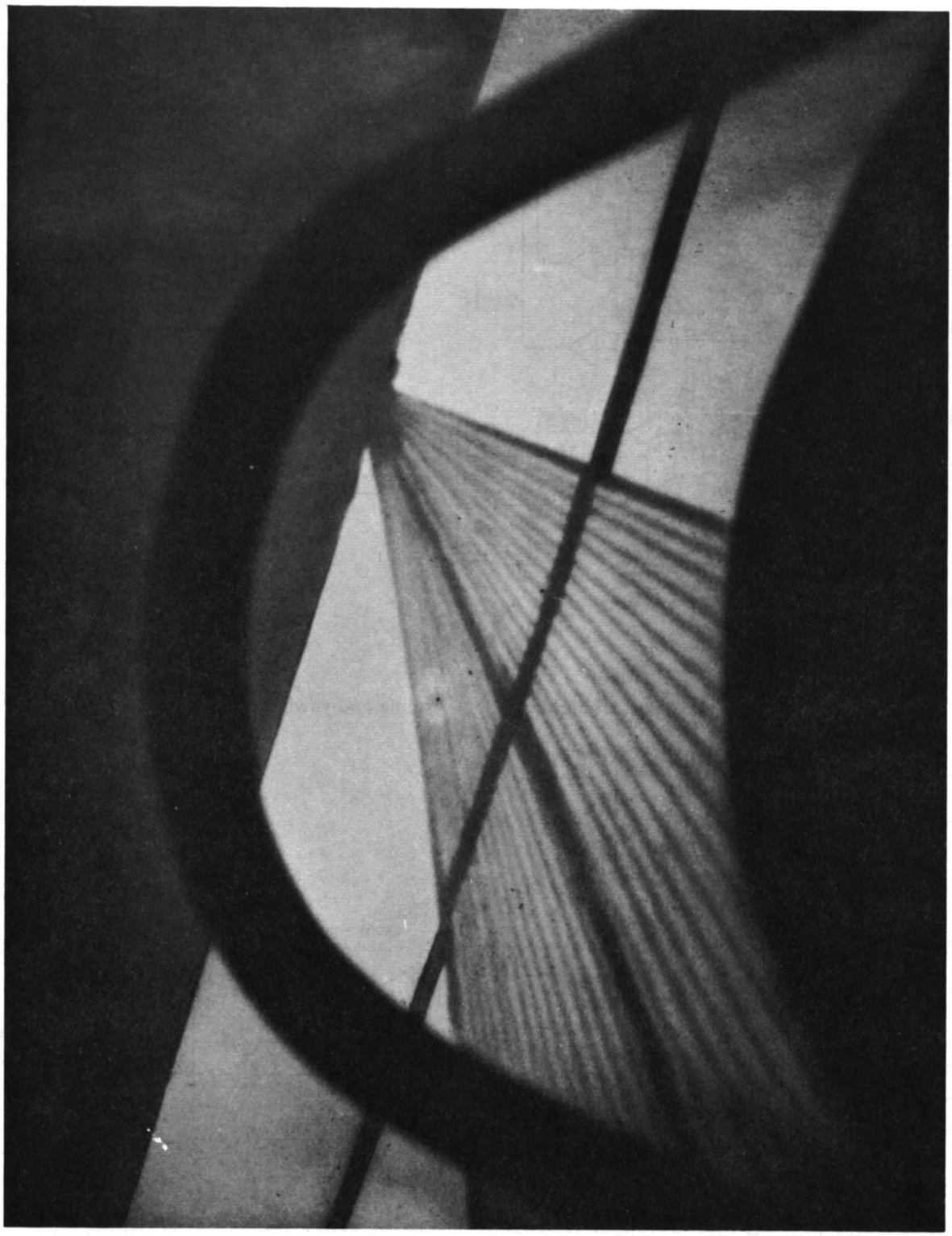

FIG. 1. Shadowgraph projection representing pilot's view of the runway.

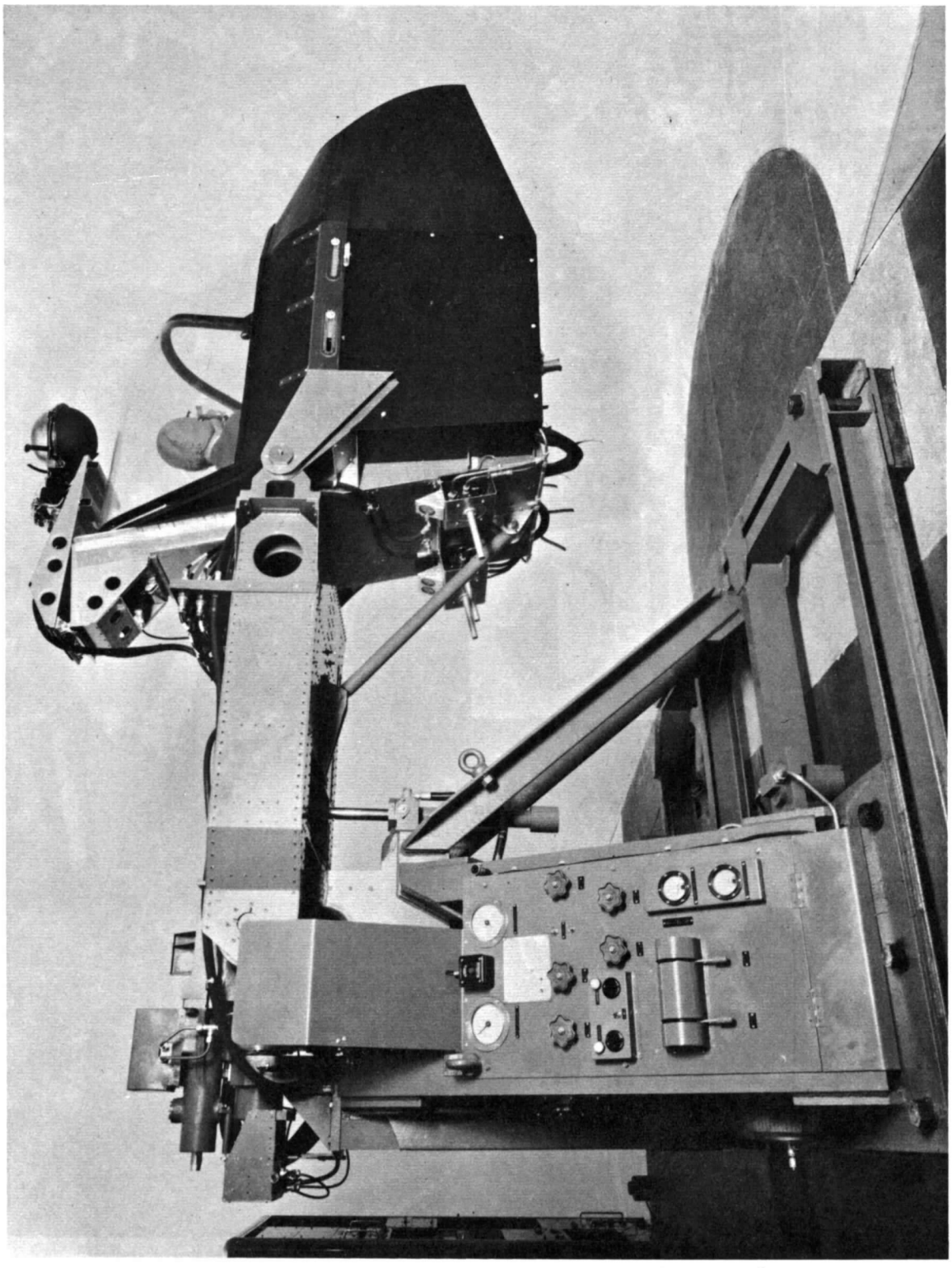

FIG. 2. Simulator cockpit and moving mechanism.

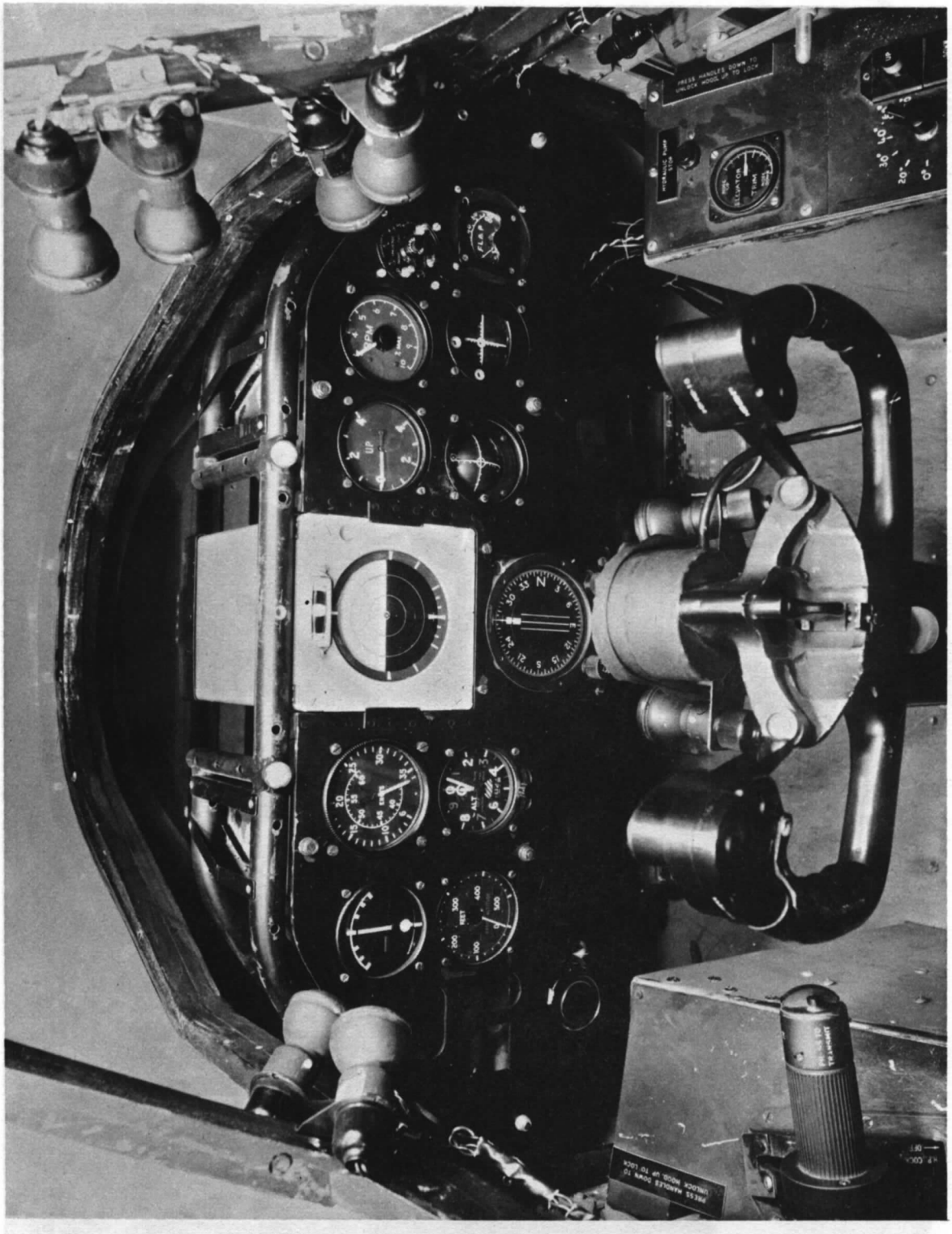

FIG. 3. Simulator flight instrument panel.

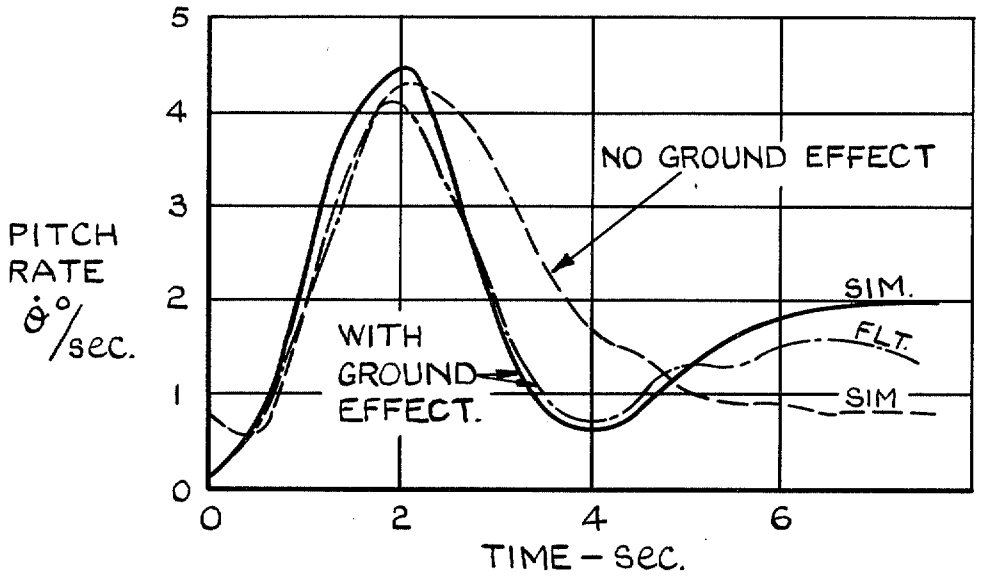

FIG. 4. Effect of ground on pitch-rate time history during take-off rotation.

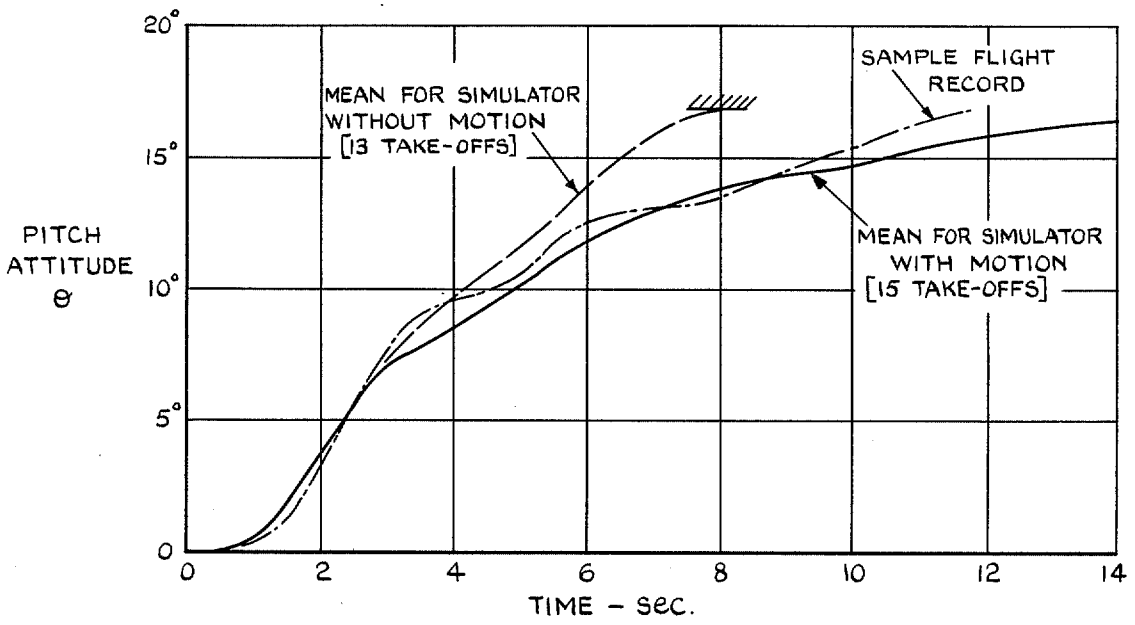

FIG. 5. Effect of simulator cockpit motion on initial climb out attitude.

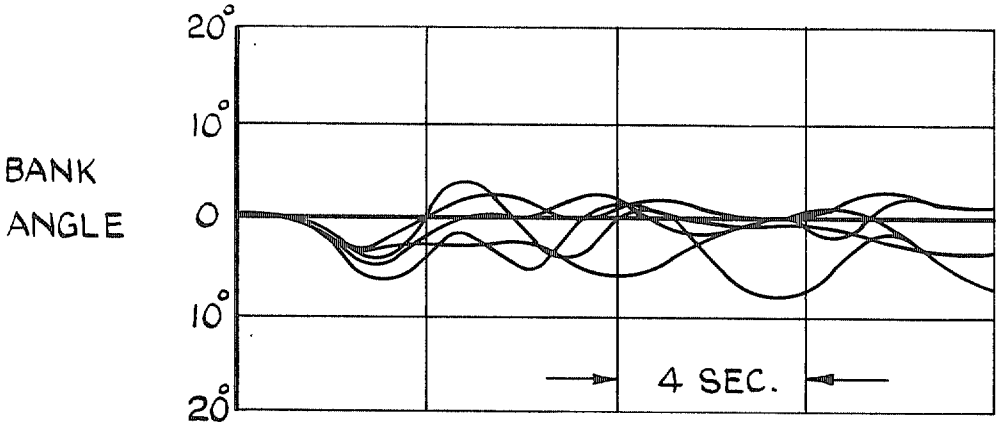

FIG. 6 (a) WITH MOTION AND VISUAL SIMULATION

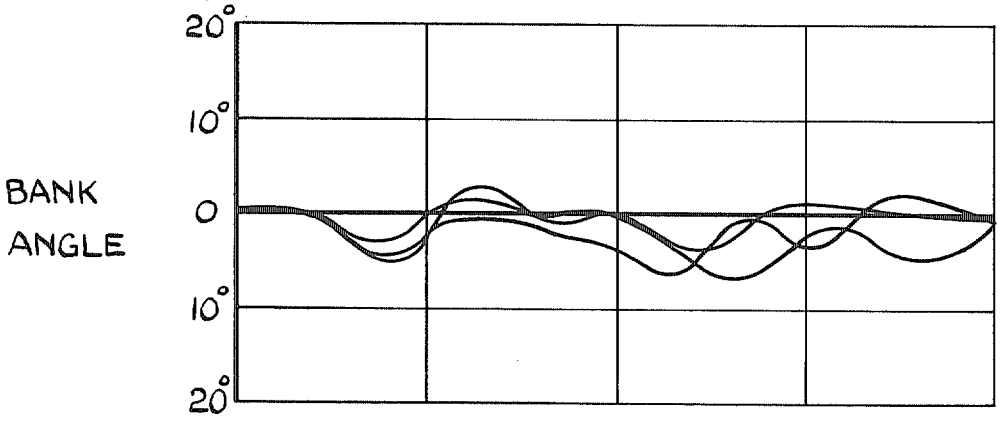

FIG. 6 (b) WITH VISUAL SIMULATION

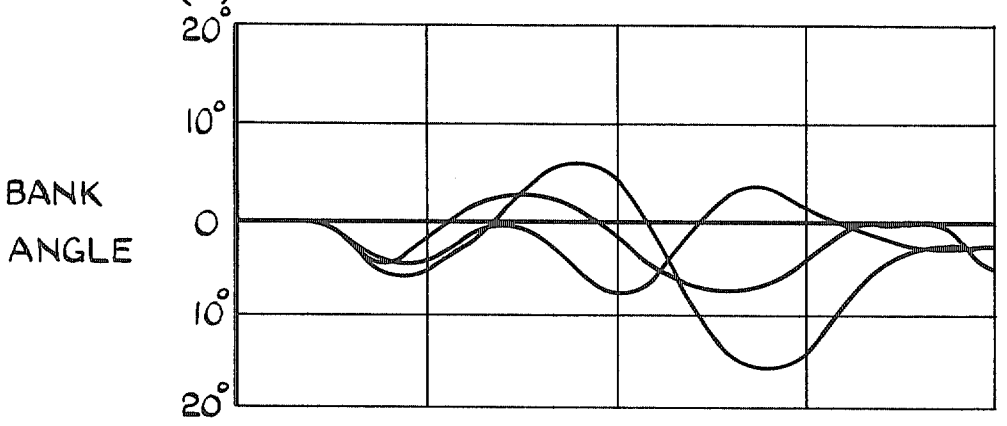

FIG. 6 (c) WITHOUT MOTION OR VISUAL SIMULATION

FIG. 6. Time histories of bank angle during simulated cross-wind take-offs. Effect of visual and motion cues.

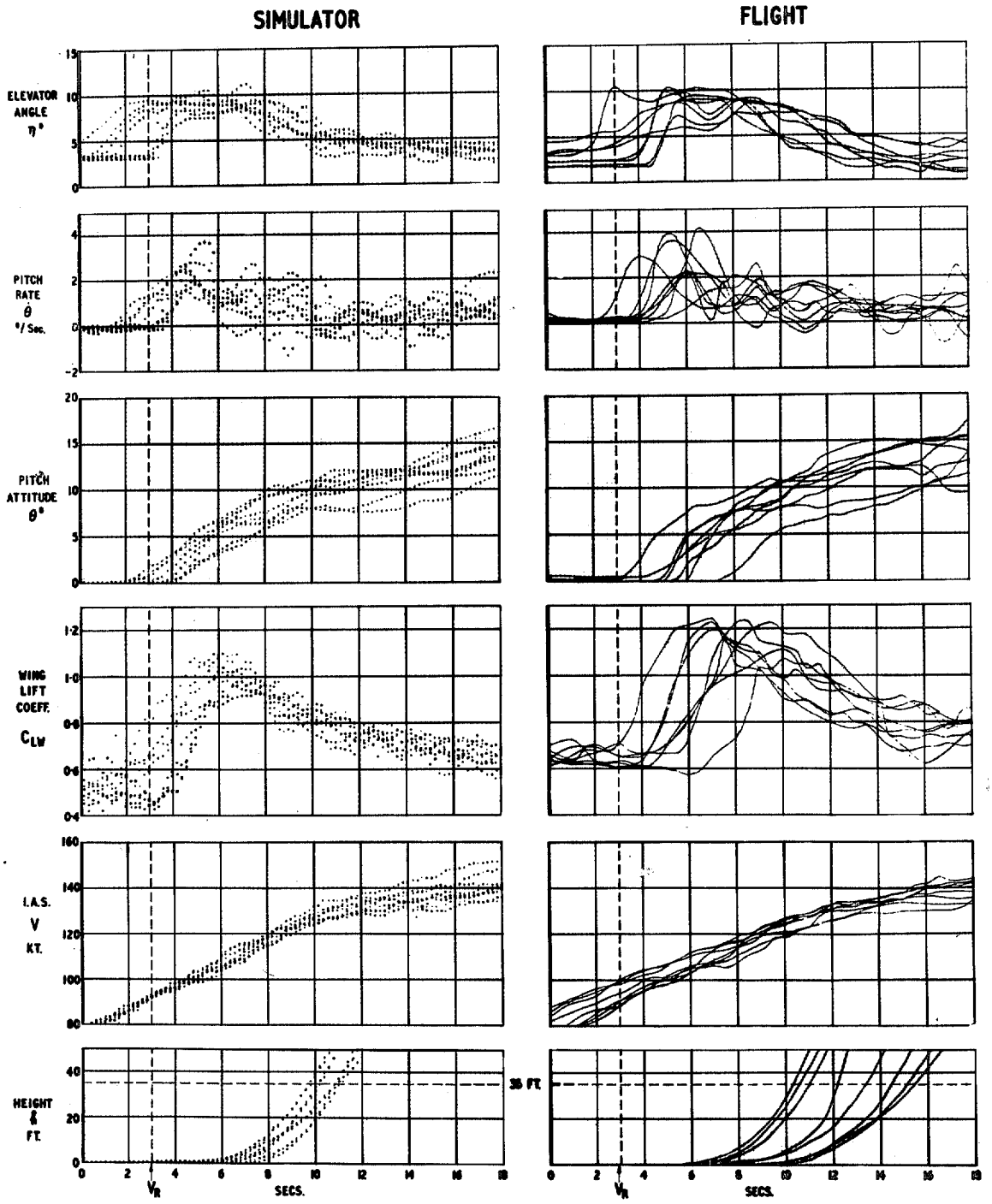

FIG. 7. Comparison of simulator and flight time histories of the rotation and flare up (with turbulence).

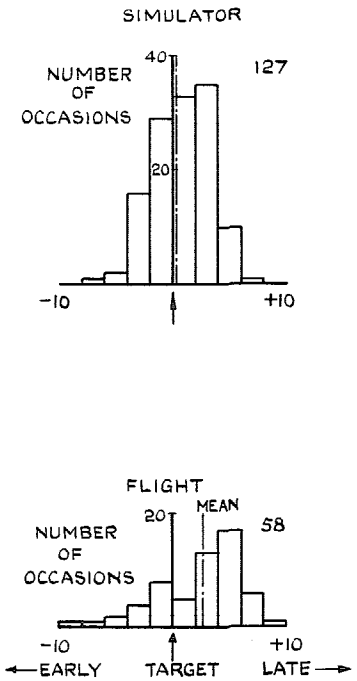

FIG. 8a. Rotation speed errors *kt*.

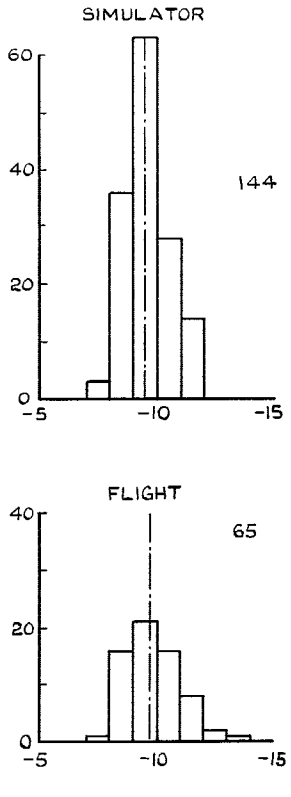

FIG. 8b. Maximum elevator angle used η^0

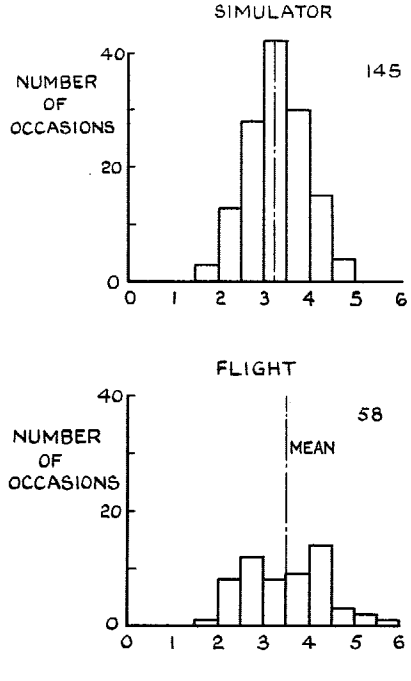

FIG. 8c. Maximum pitch rate.

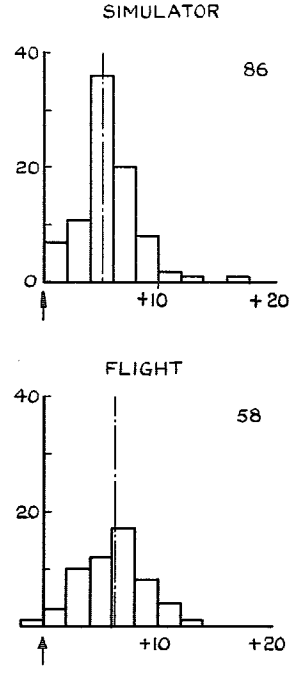

FIG. 8d. Errors from target unstick speed.

FIG. 8. Comparison of simulator and flight histograms.

FIG. 9. Director indications during the ground run.

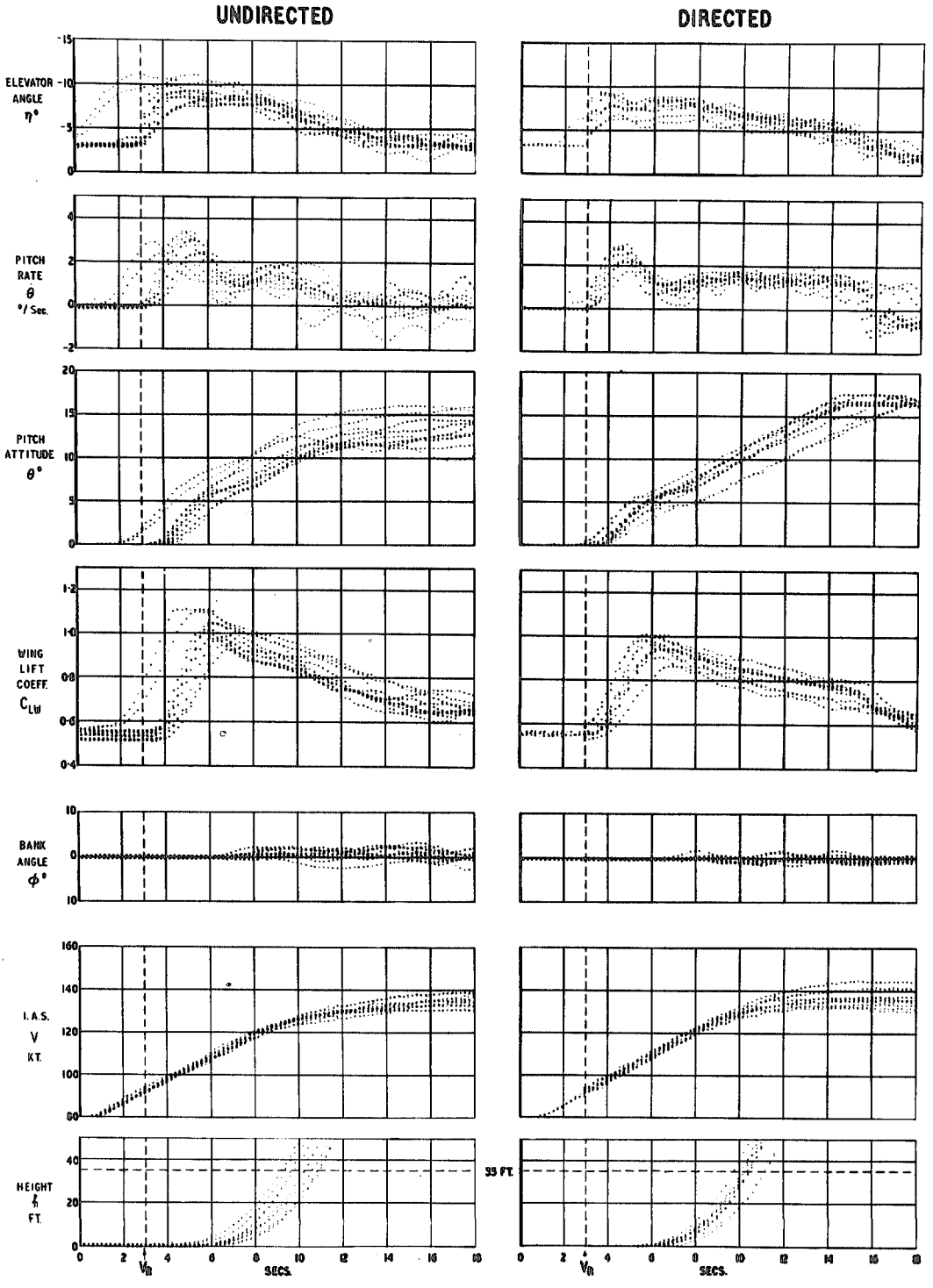

FIG. 10. Comparison of undirected and directed simulator time histories of the rotation and flare up in smooth air (code A).

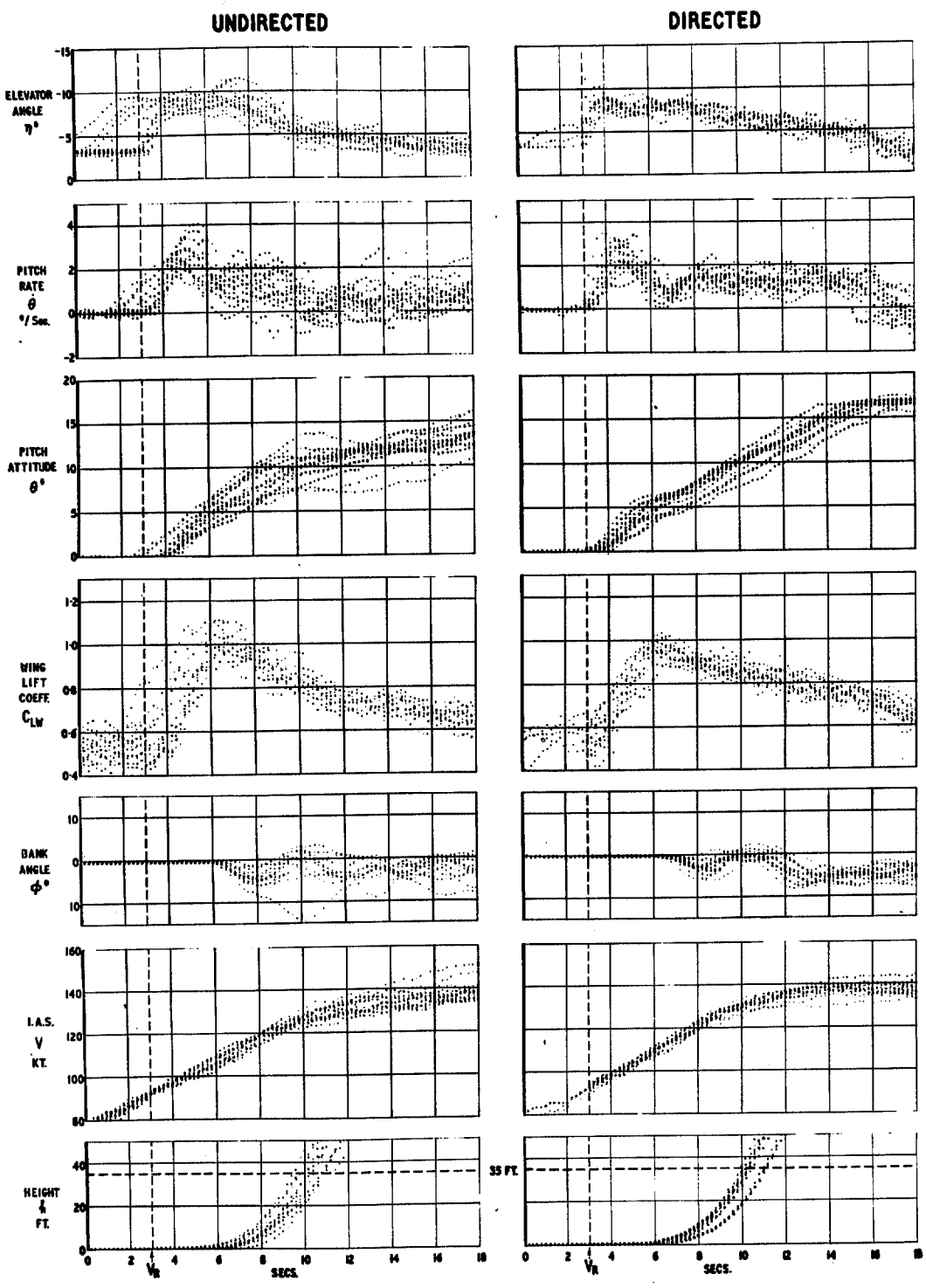

FIG. 11. Comparison of undirected and directed simulator time histories of the rotation and flare up in turbulence (code AD).

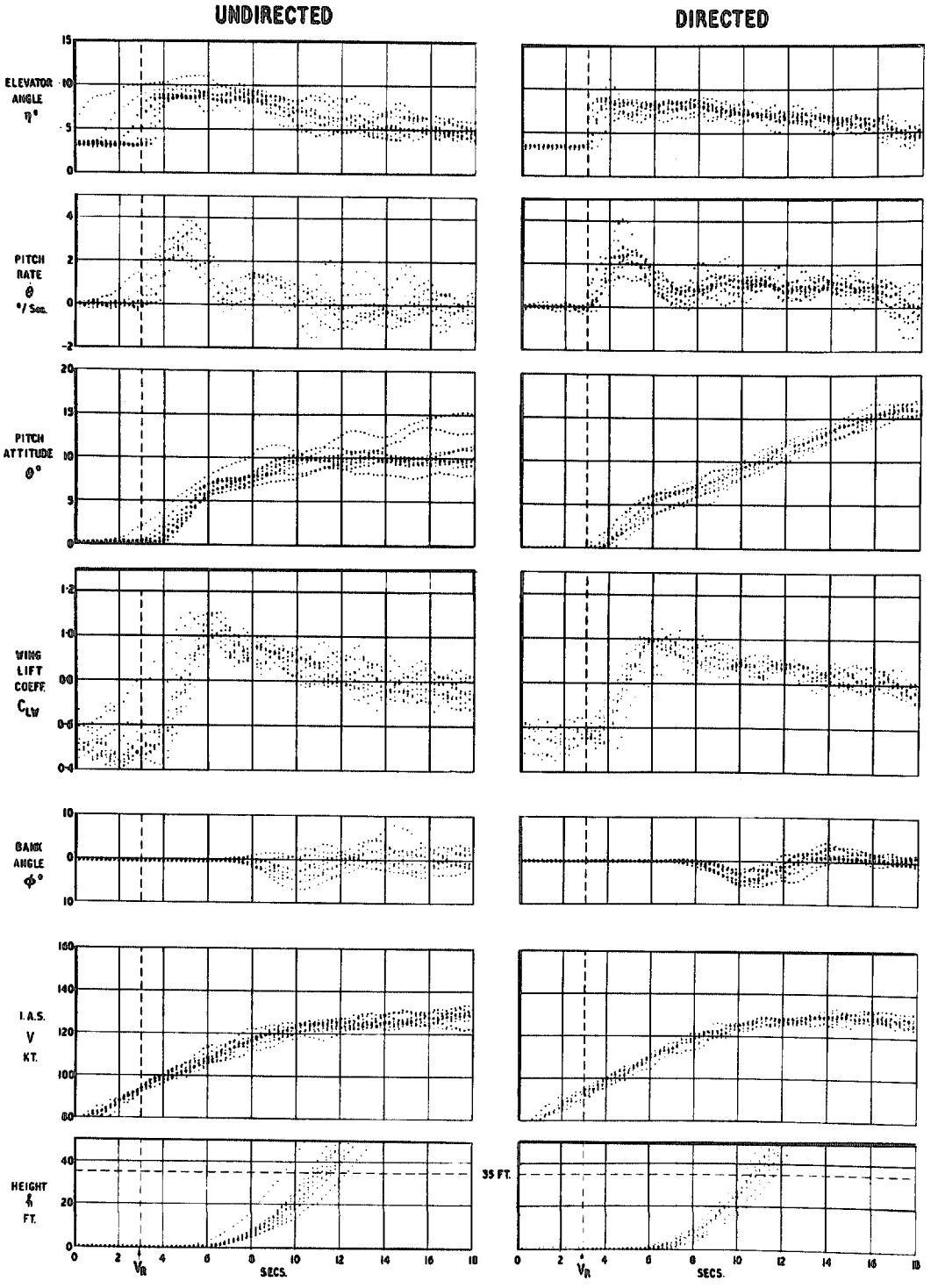

FIG. 12. Comparison of undirected and directed simulator time histories of the rotation and flare up in turbulence with engine failure at unstick (code ABD).

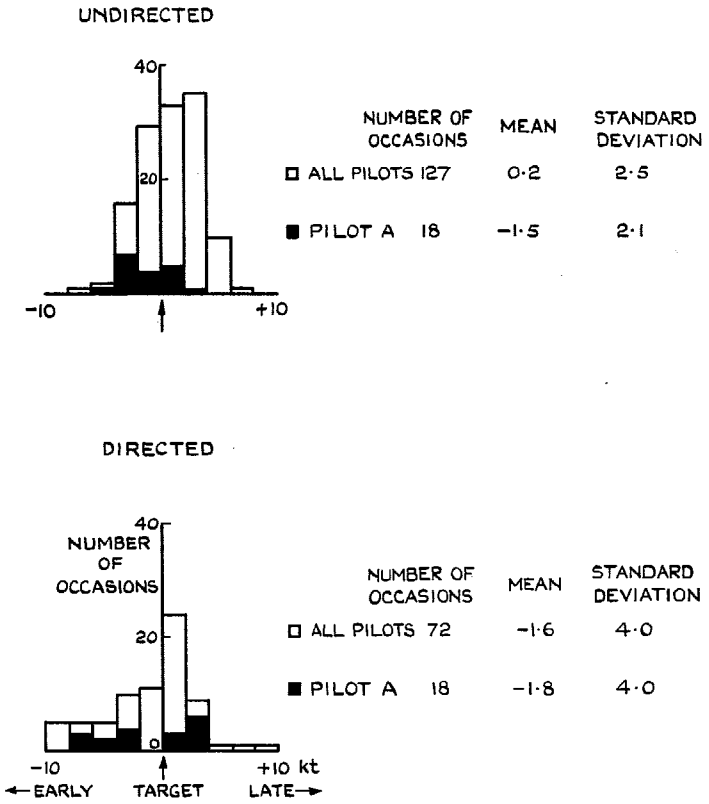

FIG. 13a. Errors in rotation speed.

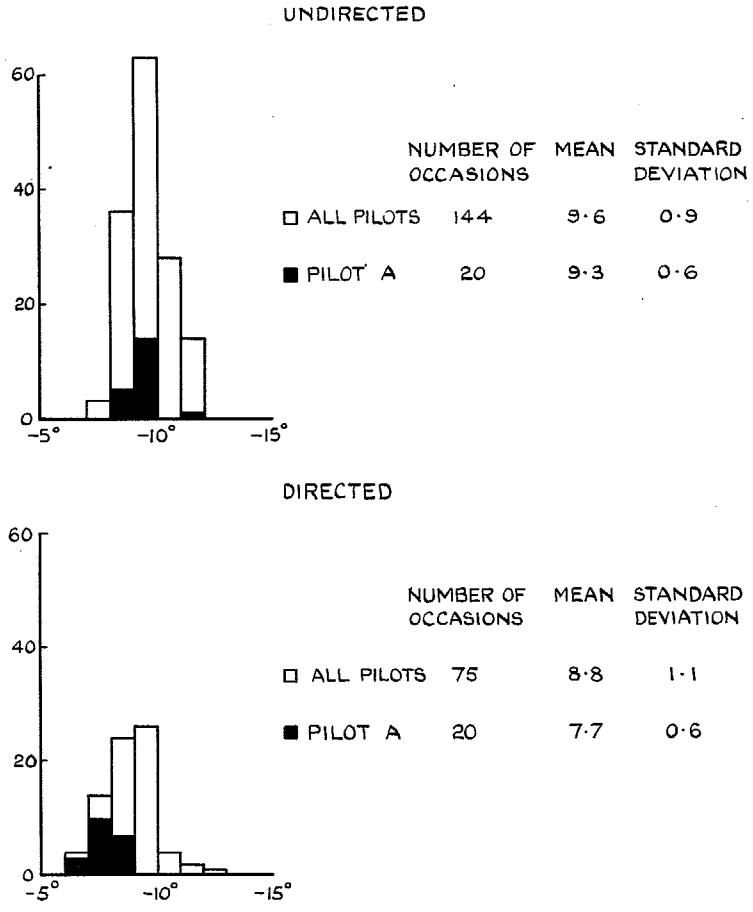

FIG. 13b. Maximum elevator used.

FIG. 13. Comparison of undirected and directed histograms.

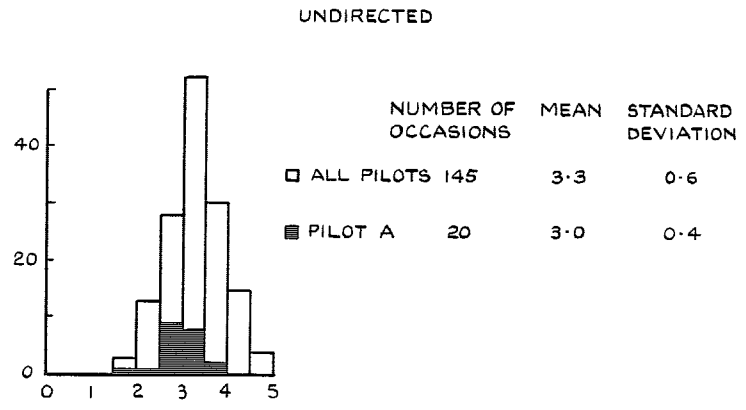

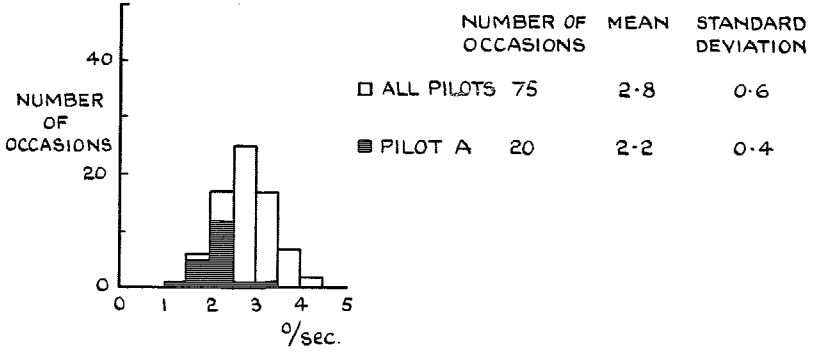

FIG. 13c. Maximum pitch rate.

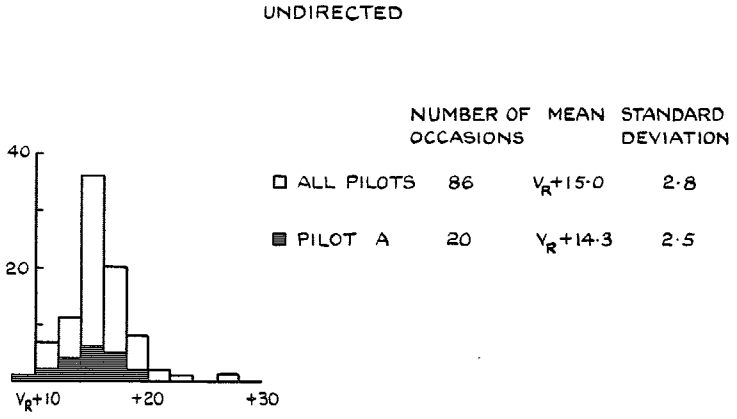

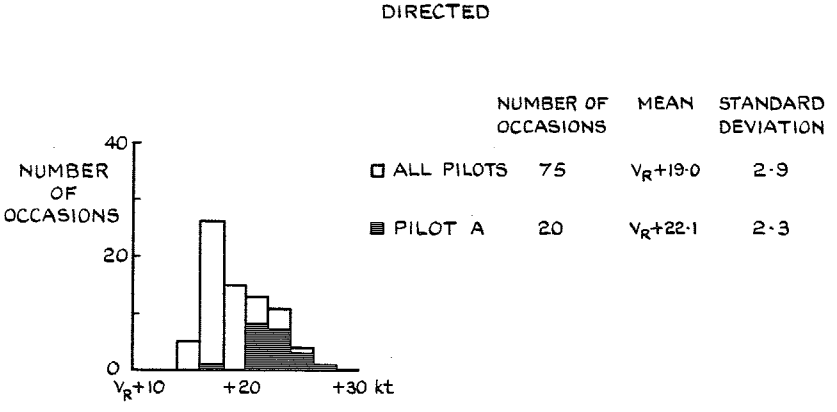

FIG. 13d. Unstick speed.

FIG. 13(contd.). Comparison of undirected and directed histograms.

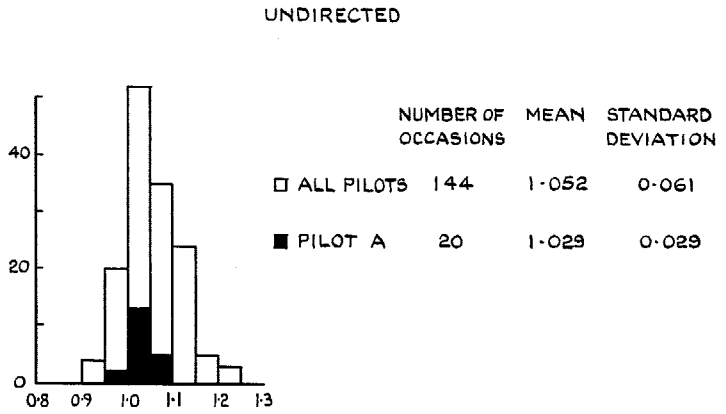

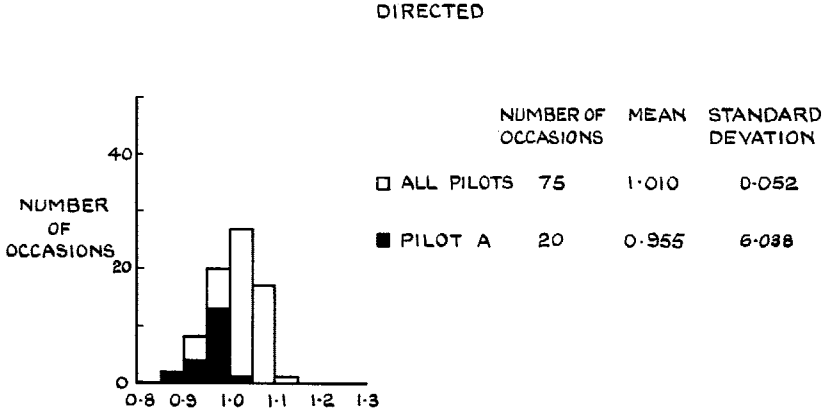

FIG. 13e. Maximum lift coefficient.

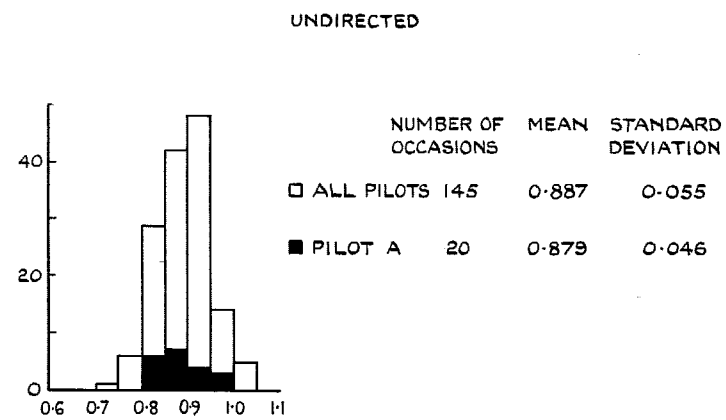

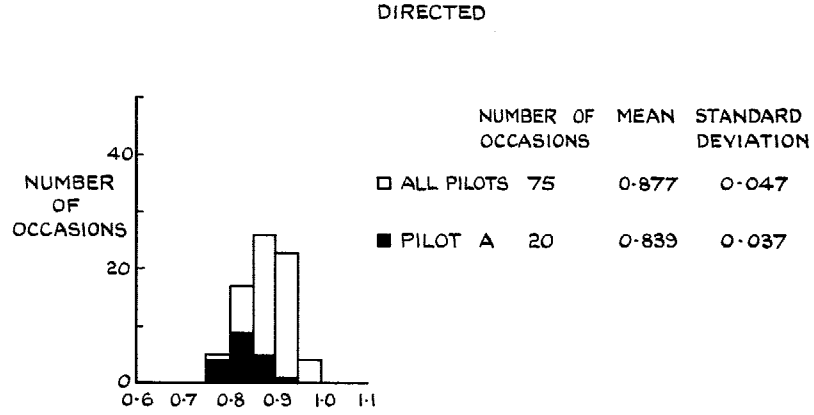

FIG. 13f. Lift coefficient at 20 ft.

FIG. 13(contd.). Comparison of undirected and directed histograms.

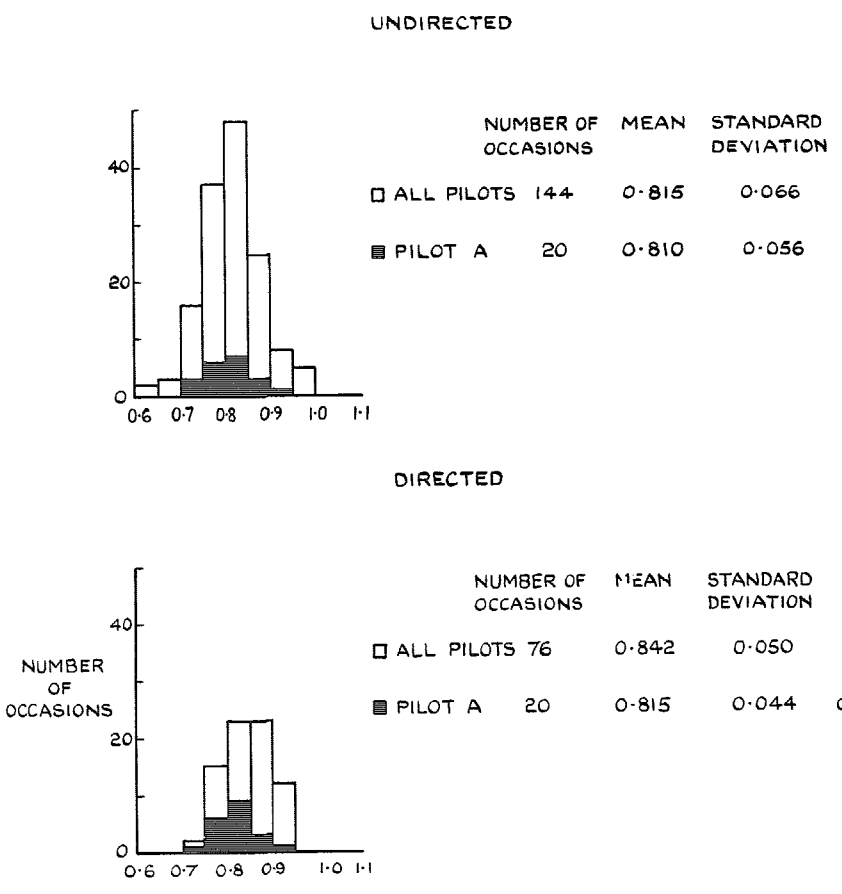

FIG. 13g. Lift coefficient at 50 ft.

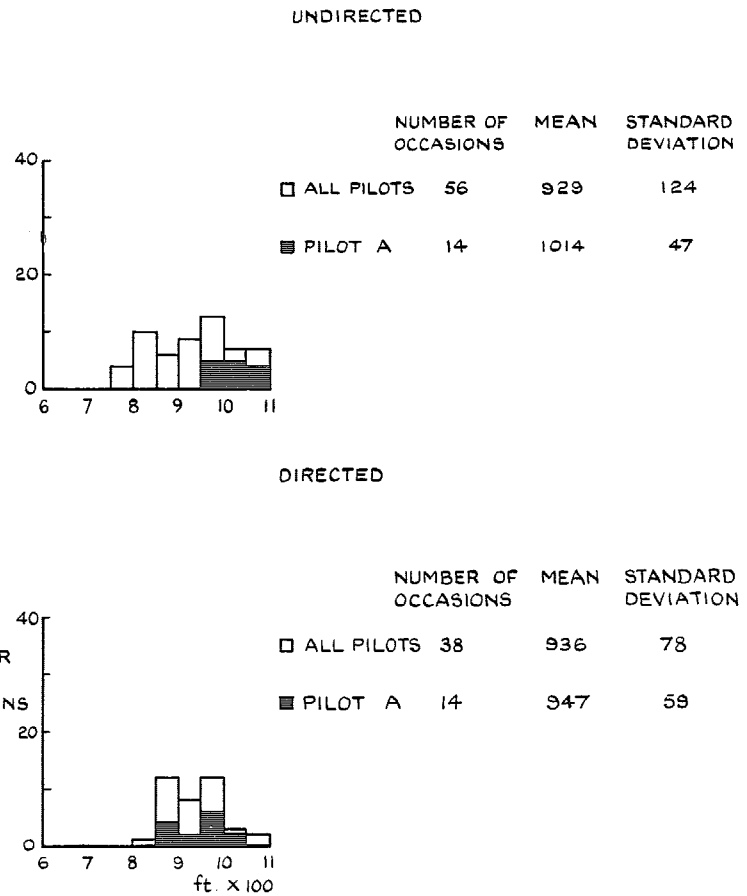

FIG. 13h. Airborne distance to reach 35 ft screen height.

FIG. 13(contd.). Comparison of undirected and directed histograms.

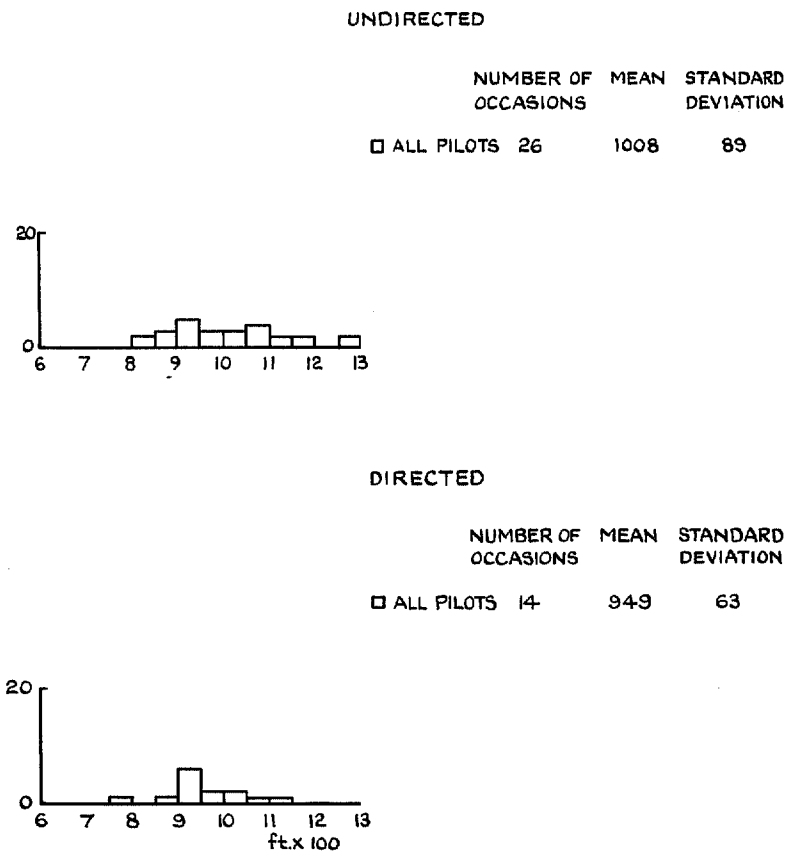

FIG. 13j. Airborne distance to reach 35 ft screen height with engine failure at unstick.

FIG. 13(concld.). Comparison of undirected and directed histograms.

Printed in Wales for Her Majesty's Stationery Office by
Allens Printers (Wales) Limited

Dd. 129527. K5.

Published by
HER MAJESTY'S STATIONERY OFFICE

To be purchased from
49 High Holborn, London W.C.1
423 Oxford Street, London W.1
13A Castle Street, Edinburgh 2
109 St. Mary Street, Cardiff CF1 1JW
Brazennose Street, Manchester 2
50 Fairfax Street, Bristol 1
258–259 Broad Street, Birmingham 1
7–11 Linenhall Street, Belfast BT2 8AY
or through any bookseller

S.O. Code No. 23 3524.